Bridging Time and Linguistics: LLMs as Time Series Analyzer through Symbolization and Segmentation

Jianyang Qin[1], **Chaoyang Li**[1,2], **Jinhao Cui**[1], **Lingzhi Wang**[1], **Zhao Liu**[2], **Qing Liao**[1,2*]
[1]Harbin Institute of Technology (Shenzhen), Shenzhen, China
[2]Pengcheng Laboratory, Shenzhen, China
`{22b351005, 22b951022, cuijinhao}@stu.hit.edu.cn,`
`{liuzhao08}@pcl.ac.cn, {wanglingzhi, liaoqing}@hit.edu.cn`

Abstract

Recent studies reveal that Large Language Models (LLMs) exhibit strong sequential reasoning capabilities, allowing them to replace specialized time-series models and serve as foundation models for complex time-series analysis. To activate the capabilities of LLMs for time-series tasks, numerous studies have attempted to bridge the gap between time series and linguistics by aligning textual representations with time-series patterns. However, it is a non-trivial endeavor to losslessly capture the infinite time-domain variability using natural language, leading to suboptimal alignment performance. Beyond representation, contextual differences, where semantics in time series are conveyed by consecutive points, unlike in text by individual tokens, are often overlooked by existing methods. To address these, we propose S^{2}TS-LLM, a simple yet effective framework to repurpose LLMs for universal time series analysis through the following two main paradigms: (i) a spectral symbolization paradigm transforms time series into frequency-domain representations characterized by a fixed number of components and prominent amplitudes, which enables a limited set of symbols to effectively abstract key frequency features; (ii) a contextual segmentation paradigm partitions the sequence into blocks based on temporal patterns and reassigns positional encodings accordingly, thereby mitigating the structural mismatch between time series and natural language. Together, these paradigms bootstrap the LLMs' perception of temporal patterns and structures, effectively bridging time series and linguistics. Extensive experiments show that S^{2}TS-LLM can serve as a powerful time series analyzer, outperforming state-of-the-art methods across time series tasks.

1 Introduction

Time series analysis [1] is widely applied across diverse domains such as transportation, energy, climate, finance, and healthcare, supporting a variety of tasks such as forecasting and classification. Owing to its practical applications, time series analysis has seen significant progress, giving rise to various specialized models tailored for certain tasks and datasets [2, 3, 4]. Recently, Large Language Models (LLMs) [5] exhibit remarkable reasoning performance, generalization ability, and multimodal knowledge, which are gradually replacing specialized models to serve as foundation models applied in various time series analysis tasks [6]. However, the inherent disparity between natural language and time series poses significant alignment challenges when leveraging LLMs for time series analysis.

The primary distinction between language and time series arises from their representational nature: natural language is composed of discrete tokens, whereas time series are continuously recorded

[*]Corresponding author

in diverse formats such as univariate or multivariate [7]. To bridge this gap, a straightforward solution is to tokenize time series as sequences of digits [8], such as representing the value 1.23 as "1", ".", "2", "3", which is inefficient in representation and fails to capture temporal dependency inherent in time series. Alternatively, other approaches [9, 7] transform time series into customized word embeddings, such as “trend” and “peak”, that are not only compatible with LLMs but also capable of capturing temporal patterns. Nevertheless, time series typically exhibit complex variations involving numerous patterns (e.g., rising, declining, stabilizing, etc.). As illustrated in Figure 1 (a), it remains a non-trivial endeavor to describe such intricate variations with concise language: the variation within the red circle requires a detailed description of its upward and downward movements, rather than being simply summarized as “relatively stable”. To address this, we propose a simple yet effective alignment paradigm, ***Spectral Symbolization***, to transform time-series patterns into textual embeddings. Technically, we apply the time-frequency transform [10] to efficiently compress time-domain sequences into compact frequency-domain representations. As depicted in the red circle in Figure 1 (b), the sparsity nature of the frequency domain enables the selection of a few dominant components to abstract temporal variations, mitigating the challenge of representing complex time-domain series accurately with natural language.

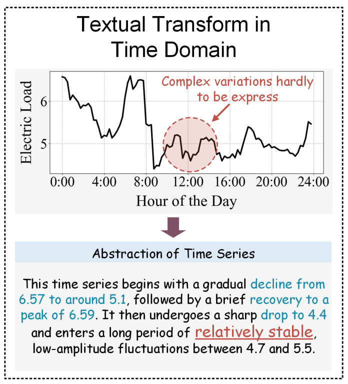

This time series begins with a gradual decline from 6.57 to around 5.1, followed by a brief recovery to a peak of 6.59. It then undergoes a sharp drop to 4.4 and enters a long period of relatively stable, low-amplitude fluctuations between 4.7 and 5.5.

(a) Time-domain

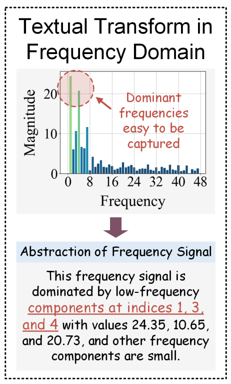

This frequency signal is dominated by low-frequency components at indices 1, 3, and 4 with values 24.35, 10.65, and 20.73, and other frequency components are small.

(b) Freq-domain

Figure 1: Illustration of the challenge in representation alignment: time-domain sequences exhibit complex variations that are hard to express concisely, whereas frequency-domain signals are typically sparse and can be captured with a few textual tokens representing dominant components.

Beyond representation differences, the discrepancy in contextual structures [11] between time series and natural language is also significant and cannot be overlooked: each token in language carries semantic meaning [12] (depicted in Figure 2 (a)); in contrast, a single time point provides limited information, with meaningful patterns emerging only across consecutive observations [13] (as shown in Figure 2 (b)). Using the token-level position encoding of standard LLMs, which assigns sequential indices to individual time points, would disrupt trend continuity (e.g., downward trend) across consecutive points, impairing the model’s awareness of temporal context. Upon this observation, we go beyond previous position processing and propose a ***Contextual Segmentation*** paradigm to align the contextual structures between natural language and time series. Specifically, we segment a sequence of time series into several blocks based on the semantic meaning between time points. As illustrated in Figure 2 (b), time points within the same block, sharing similar trend semantics, are assigned to the same positional index, allowing the LLMs to model temporal trend continuity.

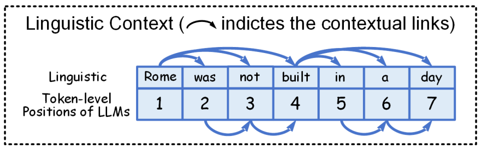
Linguistic Context (indictes the contextual links)
Linguistic
Token-level Positions of LLMs
Rome was not built in a day
1 2 3 4 5 6 7

(a) Linguistic Context

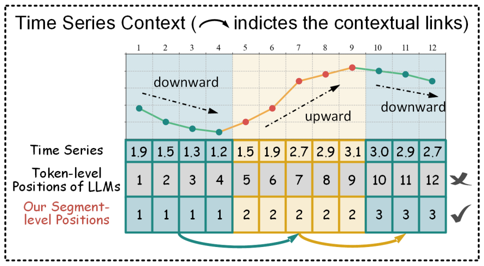

(b) Time Series Context

Figure 2: Illustration of the challenge in context alignment: standard LLMs assign positions sequentially to each token to capture context, whereas time series are better encoded by reassigning shared positions to correlated points to preserve trend continuity.

Building on these insights, we propose a novel framework, **S^{2}TS-LLM**, that repurposes the **LLM**s to align **T**ime **S**eries with the representational space and contextual structures of natural language through spectral **S**ymbolization and contextual **S**egmentation. Through these modules, we transform the time series into symbolic abstractions and segment-level positions, which are combined with the raw sequence to form a more informative input for LLMs. The temporal and textual outputs of LLMs are subsequently fused to produce predictions for downstream tasks. Our comprehensive evaluation demonstrates that S^{2}TS-LLM can serve as an effective time series analyzer, providing versatility for diverse time-series analysis tasks, such as long-term/short-term forecasting, few-shot/zero-shot learning, and classification. The main contributions of this paper are summarized as follows:

- We propose S^{2}TS-LLM, a framework that repurposes LLMs as a foundational time series analyzer by bridging the representational and contextual gaps between time series and natural language.
- The proposed spectral symbolization and contextual segmentation paradigms endow time series with frequency-based textual abstractions and language-like structural positions, bootstrapping the LLMs' comprehension of temporal variations and trend continuity.
- Extensive experiments on twenty-three datasets show that S^{2}TS-LLM can achieve performance that is comparable to or surpasses state-of-the-art methods across five major time series tasks.

2 Related Works

Time Series Analysis. Time series analysis, as a fundamental task for scientific and industrial applications, has undergone a significant revolution with the advancement of deep learning [14]. Conventional time-series models like ARIMA [15] were built upon statistical characteristics of the data, which are crafted for specific tasks. With the advent of deep learning, neural networks, such as RNNs [2], TCNs [16], MLPs [17], and Transformers [18, 19], offered task-agnostic solutions by mining the dynamic variations and long-term dependencies of time series. While these models have achieved considerable improvements, they lack generalizability across diverse time-series domains [20]. Inspired by the success of pre-training techniques in CV and NLP, recent work has explored pre-trained models for time series [21], aiming to enhance models' representation and transfer abilities across diverse domains. Although pre-training can improve models' versatility, such models remain restricted to the time-series modality, lacking sufficient data to expand their capacity and to enrich their knowledge [22]. Consequently, they fall short in handling complex real-world analytical tasks.

Large Language Models for Time Series Analysis. Compared to pre-trained models, LLMs, which acquire vast knowledge from diverse large-scale datasets, have demonstrated potential as universal analyzers applicable not only to CV and NLP but also to time series tasks [23]. Recently, a surge of LLM-based methods tailored for time series analysis has emerged [24, 25], but they inevitably face the challenge of cross-modal adaptation—transferring internal knowledge to align with time series representations [26]. Early attempts addressed this via value-to-digit conversion [23], prompt engineering [27, 28], or fine-tuning [22], yet these simplistic approaches struggle to capture temporal dependencies. Therefore, more recent work focuses on aligning textual and temporal semantics. For example, Time-LLM [9] reprograms time series into textual prototypes; CALF [5] reduces the distributional discrepancy between time-series and textual modalities in both the feature and output spaces; S^{2}IP-LLM [7] aligns decomposed components with textual anchors in a joint space; and TEST [29] applies contrastive learning to implicitly map text embeddings to temporal patterns. However, these methods rely on an unrealistic assumption that a limited set of textual tokens can faithfully represent complex and variable time-domain dynamics. Moreover, they often overlook fundamental differences in contextual structure between language and time series. To this end, this work aims to align time-series and language in the frequency domain, while reconstructing temporal contexts to better resemble textual structures.

3 Methodology

Given a sequence of textual tokens $\boldsymbol{X} = \{x_i\}_{i=1}^{l-1}$, LLMs typically encode tokens via a tokenizer $\psi(\cdot)$ and assign sequential positional indices $\boldsymbol{P} = \{p_i\}_{i=1}^{l-1}$ for tokens to generate next output tokens $\boldsymbol{Y} = \{y_i\}_{i=l}^{L}$ as follows,

$$\{\boldsymbol{y}_i\}_{i=l}^{L} = \textbf{LLMs}\left(\psi\left(\{\boldsymbol{x}_i\}_{i=1}^{l-1}\right), \{p_i\}_{i=1}^{l-1}\right), \quad \text{where} \quad p_i = i \; \forall i \in \{1, \ldots, l-1\}, \tag{1}$$

where $\psi(\cdot)$ transforms tokens into d-dimension representations. p_i indicates the position of token x_i in a sequence, allowing LLMs to capture the token's contextual dependence. When applying LLMs

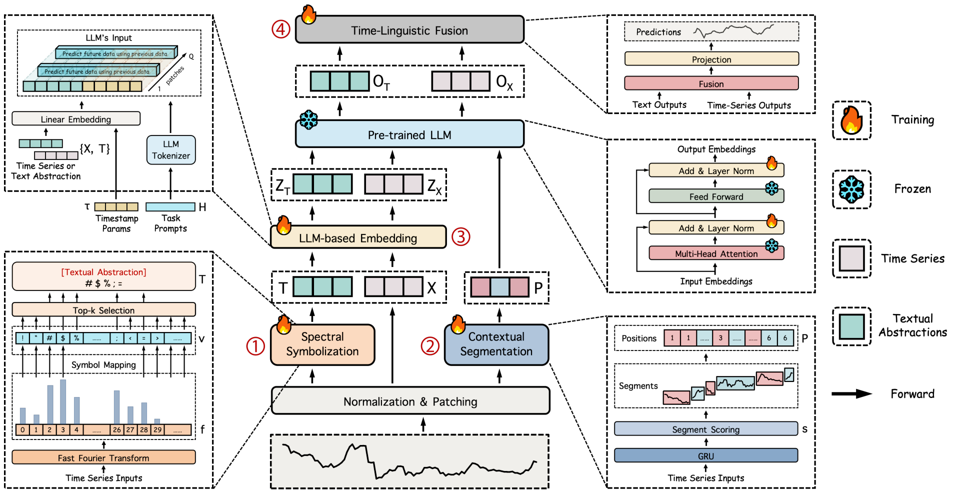

Figure 3: The framework of S^{2}TS-LLM. After processing the input time series through ① spectral symbolization and ② contextual segmentation, we obtain time-aware textual abstractions and remapped positions. ③ These, together with the time series, are embedded, packed with prompts, and fed into the pre-trained LLM. ④ The LLM outputs are fused and projected to generate predictions.

to time series analysis, the inherent gaps in representation space and contextual structure between time series and natural language hinder the models' capacity for temporal reasoning. To unlock the potential of LLMs for time series tasks, we focus on bridging time series and linguistics by (i) learning textual representations to align with time series patterns and (ii) reassigning the positional indices to alleviate the contextual mismatches.

3.1 Overview

As depicted in Figure 3, our framework encompasses four core components: (1) spectral symbolization, (2) contextual segmentation, (3) LLM-based embedding, and (4) time-linguistic fusion. Given a sequence of observations $\boldsymbol{X} \in \mathbb{R}^{N \times L}$, where $\boldsymbol{X}$ consists of N univariate time series over L time steps. Following conventional LLM-based approaches [22], we initially separate multivariate time series into N univariate series, where the n-th univariate time series is denoted as $\boldsymbol{X}^{(n)} \in \mathbb{R}^{1 \times L}$. Each univariate time series is partitioned independently into $Q = \lfloor \frac{L-M}{R} \rfloor + 1$ patches, denoted as $\hat{\boldsymbol{X}}^{(n)} \in \mathbb{R}^{Q \times M}$, using a patch size of M and a stride of R. Subsequently, these patches undergo a spectral symbolization to craft a textual abstraction $\boldsymbol{T}^{(n)}$ for representing temporal patterns, and a contextual segmentation to reassign positional indices $\boldsymbol{P}^{(n)}$ for capturing temporal context. Upon feedforwarding time series, textual abstractions and positional indices through a pre-trained LLM, we fuse the LLM's time-linguistic outputs and project them to derive the predictions $\hat{\boldsymbol{Y}}^{(n)}$ for downstream tasks such as forecasting, classification, etc., with the overall objective to minimize the errors between ground truth $\boldsymbol{Y}$ and predictions.

3.2 Spectral Symbolization

To bridge the representation gap between time series and linguistics, a common strategy is aligning time series with existing vocabulary via transformations, such as converting time series into word embeddings [24, 23] or prototypes [9, 7]. However, these transformations aim to textually represent temporal sequence in a time domain rather than frequency domain, yet they struggle to losslessly describe complex variations of time series. For example, a sequence $[66, 45, 24, 32, 27, 33, 16, 8]$ could be transformed into a textual abstraction like "*The series starts at 66 and drops to 24 over the first three points. After reaching 24, it briefly fluctuates between 32, 27, and 33, then falls again to 16 and finally 8*". While accurate, this lossless abstraction is far longer than the original sequence, reducing the efficiency of LLM learning and limiting practical applicability. In practice, a common alternative is to simplify temporal dynamics by tokenizing the same sequence merely as "*decreasing from 66 to 8*". While this achieves efficiency, it overlooks critical local variations (e.g., the intermediate fluctuations $32 \rightarrow 27 \rightarrow 33$). As such, how to textually abstract time series in a brief yet precise manner—thereby enhancing LLMs' temporal comprehension—remains an open issue.

To achieve this, we propose a spectral symbolization paradigm that transforms frequency-domain patterns of time series $\hat{\boldsymbol{X}}^{(n)} \in \mathbb{R}^{Q \times M}$ into symbolic sequences, rather than modeling time-domain features. Technically, a time series can be expressed as a superposition of sine waves characterized by various frequencies through Fast Fourier Transform (FFT) [10],

$$\left[f_{q,1}, f_{q,2}, \cdots, f_{q,\lfloor \frac{M}{2} \rfloor}\right] = \text{FFT}\left(\hat{\boldsymbol{X}}_q^{(n)}\right), \tag{2}$$

where $\hat{\boldsymbol{X}}_q^{(n)}$ is the q-th patch of time series and $f_{q,*}$ denotes a specific frequency. $\lfloor \frac{M}{2} \rfloor$ is the number of frequencies, equal to half of the dimensions M because of the symmetry of FFT. Compared to time-domain data, frequency-domain signals are typically sparse and dominated by a few components, which helps reduce noise caused by complex temporal variations [13]. The compact nature of frequency allows us to use a finite and fixed set of textual tokens for time-series representation,

$$\left[v_1, v_2, \cdots, v_{\lfloor \frac{M}{2} \rfloor}\right] \longleftarrow \left[f_{q,1}, f_{q,2}, \cdots, f_{q,\lfloor \frac{M}{2} \rfloor}\right], \tag{3}$$

where v_m is the m-th textual token corresponding to $f_{q,m}$. To distinguish time series representation between patches, we further identify salient textual tokens from $\left[v_1, \cdots, v_{\lfloor \frac{M}{2} \rfloor}\right]$ for each patch $\hat{\boldsymbol{X}}_q^{(n)}$ to describe its unique patterns. Specifically, we select the textual tokens corresponding to the top-k frequencies with the highest amplitudes to form an abstraction of the time series, denoted as $\boldsymbol{T}_q^{(n)} = \{v_i\}_{i=1}^k$,

$$\{v_1, v_2, \cdots, v_k\} \underset{k \in \{1, \cdots, \lfloor \frac{M}{2} \rfloor\}}{\longleftarrow} \{f_{q,1}, f_{q,2}, \cdots, f_{q,k}\} = \underset{k \in \{1, \cdots, \lfloor \frac{M}{2} \rfloor\}}{\text{argTopk}} \left(\text{Amp}\left(\text{FFT}\left(\hat{\boldsymbol{X}}_q^{(n)}\right)\right)\right) \tag{4}$$

where $\text{Amp}(\cdot)$ represents the calculation of amplitude values. $\{f_{q,1}, f_{q,2}, \cdots, f_{q,k}\}$ are top-k frequency components selected from the q-th data patch. Although these top-k frequencies carry relatively compact information, they are capable of capturing the global patterns of a time series[30, 31, 32], supporting an effective characterization of the sequence. For instance, given the same sequence $[66, 45, 24, 32, 27, 33, 16, 8]$ mentioned above, using the top-2 frequency components can reconstruct a sequence $[57, 36, 14, 33, 32, 46, 23, 10]$ that preserves the original trend of "decreasing→fluctuating→decreasing".

For mapping a frequency $f_{q,k}$ to a token v_k, one straightforward approach is to assign predefined textual vocabulary (such as "trend" and "peak") to each frequency based on the datasets and tasks. However, this requires labor-intensive manual selection and lacks generalizability across different settings. As an alternative, we choose the first $\lfloor \frac{M}{2} \rfloor$ ASCII symbols (e.g., "@", "!", or "+") to describe corresponding $\lfloor \frac{M}{2} \rfloor$ frequencies. Although these symbols do not carry explicit semantics, LLMs can use the statistical properties learned during pretraining [33, 34, 35] to interpret them like a foreign language, associating different symbol combinations with distinguishable spectral patterns. Consequently, the mapped top-k textual tokens $\{v_1, v_2, \cdots, v_k\}$ provides concise yet unambiguous cues that enable LLMs distinguish global time-series trends such as periodicity, volatility, or smoothness. In this paper, we implement the model using the ASCII symbol mapping scheme, while the implementation details and results of the predefined vocabulary mapping are additionally reported in the Appendix E.6.

3.3 Contextual Segmentation

Due to the contextual discrepancy between time series and natural language, the token-level position encoding assigns sequential indices to time-series patches (as shown in Eq. 1), which hinders LLMs from capturing temporal trend continuity, such as downward and upward movements. To address this, we propose a contextual segmentation paradigm that dynamically partitions a sequence of Q patches into several blocks and assigns a positional index to each block. Regarding an input time series $\hat{\boldsymbol{X}}^{(n)} = \left[\hat{\boldsymbol{x}}_1^{(n)}, \cdots, \hat{\boldsymbol{x}}_Q^{(n)}\right]$, we first pass it through a GRU to get hidden embeddings $\left\{\boldsymbol{c}_q^{(n)}\right\}_{q=1}^Q$, and then calculate their segment score $\boldsymbol{s}$ through ℓ_2-distance,

$$\left\{\boldsymbol{c}_q^{(n)}\right\}_{q=1}^Q = \text{GRU}\left(\left\{\hat{\boldsymbol{x}}_q^{(n)}\right\}_{q=1}^Q\right), \quad \boldsymbol{s}(i,j) = \|\boldsymbol{c}_i^{(n)} - \boldsymbol{c}_j^{(n)}\|_2. \tag{5}$$

Intuitively, the score $\boldsymbol{s}(i,j)$ determines whether the patches i and j should belong to the same block: if $\boldsymbol{s}(i,j) < \gamma$, they are grouped together; otherwise, they are separated. After obtaining B segments, we assign sequential positional indices $\boldsymbol{P}^{(n)}$ from 1 to B to the resulting segments. Here, we provide an intuitive example to illustrate the difference between our segment-level position and token-level position encoding of standard LLMs: given a time series with 6 patches, conventional token-level encoding assigns sequential indices $[1,2,3,4,5,6]$, whereas our approach may assign grouped indices like $[1,1,1,2,2,3]$ to better reflect structural continuity. These segment-level positions are subsequently fed into the LLMs to enhance the model's awareness of temporal context. Notably, segmentation is used solely for reassigning positions and does not alter the input time series itself.

3.4 LLM-based Embedding

Given the time series $\hat{\boldsymbol{X}}^{(n)}$ and learned textual abstraction $\boldsymbol{T}^{(n)}$, we embed them using a simple linear layer $\phi(\cdot)$ and concatenate them with a learnable timestamp parameter $\boldsymbol{\tau}$,

$$\boldsymbol{E}_X^{(n)} = \phi(\boldsymbol{X}^{(n)}) \oplus \boldsymbol{\tau}, \quad \boldsymbol{E}_T^{(n)} = \phi(\boldsymbol{T}^{(n)}) \oplus \boldsymbol{\tau}. \tag{6}$$

Then, inspired by success of prompt engineering [36], we augment the embeddings $\boldsymbol{E}_X^{(n)}$ and $\boldsymbol{E}_T^{(n)}$ with task-specific prompts $\boldsymbol{H}$ (e.g., "*Predict future sequences using previous data*" for forecasting task) as LLMs' input tokens $\boldsymbol{Z}_X^{(n)}$ and $\boldsymbol{Z}_T^{(n)}$. Regarding that an embedding $\boldsymbol{E}_* \in \{\boldsymbol{E}_X, \boldsymbol{E}_T\} = [\boldsymbol{e}_{*,1}, \boldsymbol{e}_{*,2}, \cdots, \boldsymbol{e}_{*,B}]$ is divided into B blocks through contextual segmentation and a prompt $\boldsymbol{H} = [h_1, h_2, \cdots, h_W]$ has W words, we split the embeddings into G slices and insert the prompt at the end of each slice as follows,

$$\boldsymbol{Z}_*^{(n)} = \left\{ \boldsymbol{e}_{*,g\times U+1}^{(n)}, \cdots, \boldsymbol{e}_{*,g\times U+U}^{(n)}, \boldsymbol{h}_1, \cdots, \boldsymbol{h}_W \mid g \in [0,1,\cdots,G-1],\ U = \lfloor \frac{B}{G} \rfloor \right\}. \tag{7}$$

The token sequences $\boldsymbol{Z}_X^{(n)}$ and $\boldsymbol{Z}_X^{(n)}$ are processed by a shared backbone LLM with segment-level positional indices $\boldsymbol{P}^{(n)}$, yielding the output representations $\boldsymbol{O}_X^{(n)}$ and $\boldsymbol{O}_T^{(n)}$, respectively. Following common fine-tuning practices for LLMs [22], we freeze all components of the LLMs except for Layer Normalization (LN) layers, allowing time series adaptation.

3.5 Time-Linguistic Fusion

As the textual output $\boldsymbol{O}_T^{(n)}$ represent frequency-domain patterns distinct from the time-domain output $\boldsymbol{O}_X^{(n)}$, we treat $\boldsymbol{O}_T^{(n)}$ as a complementary guide and dynamically integrate it with $\boldsymbol{O}_X^{(n)}$ via a gated residual update, ensuring that predictions remain in the time domain:

$$\boldsymbol{O}^{(n)} = \boldsymbol{O}_X^{(n)} + \boldsymbol{A}^{(n)} \odot \sigma(\boldsymbol{O}_T^{(n)}) \odot \boldsymbol{O}_X^{(n)}, \quad \boldsymbol{A}^{(n)} = \frac{\boldsymbol{O}_T^{(n)} \boldsymbol{O}_X^{(n)}}{\|\boldsymbol{O}_T^{(n)}\| \|\boldsymbol{O}_X^{(n)}\|}. \tag{8}$$

Here, $\sigma(\cdot)$ denotes a sigmoid activation that nonlinearly transforms spectral features, serving as a gating signal [37] to leverage frequency information in controlling which components of the time-domain signal are preserved or suppressed. The cosine similarity $\boldsymbol{A}^{(n)}$ further modulates the fusion, emphasizing time-domain components that are semantically aligned with frequency-domain patterns. Finally, the fused outputs $\boldsymbol{O}^{(n)}$ are processed through prefix truncation [9], flattening, and a linear projection to produce the final prediction $\hat{\boldsymbol{Y}}^{(n)}$.

4 Experiments

To evaluate the model's effectiveness, we adhere to the experimental settings in [22] and conduct extensive experiments on five mainstream analysis tasks, including long/short-term forecasting, few-shot/zero-shot learning, and time-series classification. As shown in Figure 4, experimental results demonstrate that S^{2}TS-LLM[1] achieves performance comparable to or surpassing state-of-the-art models across diverse downstream tasks.

[1]https://github.com/JianyangQin/S2TS-LLM

Baselines. We compare our method against a series of well-known and advanced baselines, including LLM-based models (S^{2}IP-LLM [7], Time-LLM [9], GPT4TS [22]), Transformer-based models (TimeXer [38], iTransformer [39], PatchTST [40]), MLP-based models (TimeMixer [41], RLinear [17]), and a CNN-based model (TimesNet [13]). Notably, we uniformly use GPT-2 [42] as the backbone of all LLM-based models for fair comparison. Besides, a broader set of models is further employed for classification comparison. More experimental details are shown in Appendix B.

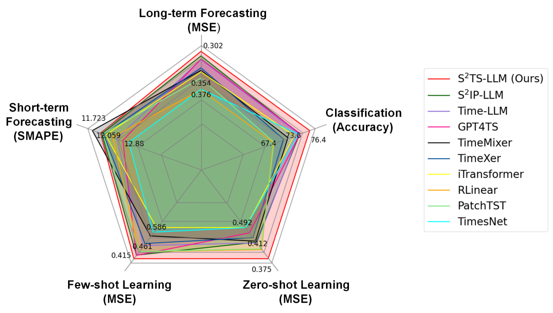

Figure 4: Overall Model Comparison.

4.1 Long-term Forecasting

Setups. We perform long-term forecasting on Weather, Electricity (ECL), Traffic, ETTh1, ETTh2, ETTm1, and ETTm2 datasets [13]. Following the experimental settings commonly used in LLM-based methods [22], the input time series length L is set to 512, and the forecasting performance is evaluated across four prediction horizons {96, 192, 336, 720}, using Mean Squared Error (MSE) and Mean Absolute Error (MAE) as evaluation metrics.

Results. A summary of the forecasting results is presented in Table 1. Due to the expressive power of LLMs, LLM-based models, including our method, S^{2}IP-LLM, Time-LLM, and GPT4TS, generally outperform conventional baselines, highlighting the potential of LLMs in time series reasoning. Notably, while our method shares a similar goal of aligning time series with LLMs' textual representations as S^{2}IP-LLM and Time-LLM, our method consistently outperforms them. These improvements are mainly attributed to the following factors: (1) the spectral symbolization paradigm is capable of capturing frequency patterns, mitigating the difficulty of representing complex time-domain dynamics with discrete tokens; and (2) we further align contextual structures between time series and language, enhancing the LLMs' comprehension of sequential dependencies.

4.2 Short-term Forecasting

Setups. We conduct short-term forecasting using the M4 dataset [43], which comprises 100,000 time series sampled at various frequencies including yearly, quarterly, monthly, weekly, daily, and hourly. In this case, prediction horizons range from 6 to 48, with input lengths set to twice the prediction horizon. For evaluation, we adopt Symmetric Mean Absolute Percentage Error (SMAPE), Mean Absolute Scaled Error (MASE), and Overall Weighted Average (OWA) as metrics.

Results. As shown in Table 2, conventional specialized models, such as TimeMixer and PatchTST exhibit more impressive performance over LLM-based methods in short-term forecasting. A plausible explanation is that short input lengths constrain the statistical inference capabilities of LLMs. For example, the yearly subset of the M4 dataset provides only 12 time steps of data as input, offering insufficient long-term dependency; thus, LLMs are prone to overfit local noise rather than capture global statistical patterns. Nevertheless, our S^{2}TS-LLM still achieves competitive suboptimal performance, benefiting from its effective spectral representation and contextual learning capabilities.

Table 1: Long-term forecasting results. All the results are averaged from four different prediction horizons $\{96, 192, 336, 720\}$. Red denotes the best performance, while Blue indicates the second-best. Detailed results are provided in Appendix E.1.

Methods	**S^{2}TS-LLM (Ours)**		S^2 IP-LLM [7]		Time-LLM [9]		GPT4TS [22]		TimeMixer [41]		TimeXer [38]		iTransformer [39]		RLinear [17]		PatchTST [40]		TimesNet [13]	
Metric	MSE ↓	MAE ↓	MSE ↓	MAE ↓	MSE ↓	MAE ↓	MSE ↓	MAE ↓	MSE ↓	MAE ↓	MSE ↓	MAE ↓	MSE ↓	MAE ↓	MSE ↓	MAE ↓	MSE ↓	MAE ↓	MSE ↓	MAE ↓
Weather	0.225	0.265	0.228	0.265	0.237	0.269	0.237	0.270	0.240	0.271	0.241	0.271	0.258	0.278	0.272	0.291	0.259	0.281	0.259	0.287
ECL	0.164	0.256	0.166	0.262	0.167	0.264	0.167	0.263	0.182	0.272	0.171	0.270	0.178	0.270	0.219	0.298	0.216	0.304	0.192	0.295
Traffic	0.396	0.278	0.405	0.286	0.407	0.289	0.414	0.294	0.484	0.297	0.466	0.287	0.428	0.282	0.626	0.378	0.481	0.304	0.620	0.336
ETTh1	0.404	0.429	0.418	0.436	0.426	0.435	0.427	0.426	0.447	0.440	0.437	0.437	0.454	0.447	0.446	0.434	0.469	0.454	0.458	0.450
ETTh2	0.321	0.376	0.355	0.399	0.361	0.398	0.354	0.394	0.364	0.395	0.367	0.396	0.383	0.407	0.374	0.398	0.387	0.407	0.414	0.427
ETTm1	0.344	0.380	0.346	0.382	0.354	0.384	0.352	0.383	0.381	0.395	0.382	0.397	0.407	0.410	0.414	0.407	0.387	0.400	0.400	0.406
ETTm2	0.258	0.318	0.262	0.326	0.275	0.334	0.266	0.326	0.275	0.323	0.274	0.322	0.288	0.332	0.286	0.327	0.281	0.326	0.291	0.333
Average	0.302	0.329	0.311	0.337	0.318	0.339	0.317	0.337	0.339	0.342	0.334	0.340	0.342	0.347	0.377	0.362	0.353	0.352	0.376	0.362

Table 2: Short-term forecasting results. The SMAPE, MASE, OWA results are weighted averaged across all M4 datasets, with prediction horizons ranging from $[6, 48]$. Red denotes the best performance, while Blue indicates the second-best. Detailed results are provided in Appendix E.2.

Methods	**S^{2}TS-LLM (Ours)**	S^{2}IP-LLM [7]	Time-LLM [9]	GPT4TS [22]	TimeMixer [41]	TimeXer [38]	iTransformer [39]	RLinear [17]	PatchTST [40]	TimesNet [13]
SMAPE ↓	11.979	12.021	12.494	12.690	11.723	12.082	12.142	12.363	12.059	12.880
MASE ↓	1.610	1.612	1.731	1.808	1.559	1.621	1.631	1.662	1.623	1.836
OWA ↓	0.862	0.857	0.913	0.940	0.840	0.874	0.869	0.890	0.869	0.955

Table 3: Few-shot learning results on 5% and 10% training data. Detailed results are provided in Appendix E.3.

Volume	Methods	**S^{2}TS-LLM (Ours)**		S^{2}IP-LLM [7]		Time-LLM [9]		GPT4TS [22]		TimeMixer [41]		TimeXer [38]		iTransformer [39]		RLinear [17]		PatchTST [40]		TimesNet [13]	
	Metric	MSE ↓	MAE ↓	MSE ↓	MAE ↓	MSE ↓	MAE ↓	MSE ↓	MAE ↓	MSE ↓	MAE ↓	MSE ↓	MAE ↓	MSE ↓	MAE ↓	MSE ↓	MAE ↓	MSE ↓	MAE ↓	MSE ↓	MAE ↓
5%	ETTh1	0.580	0.503	0.650	0.550	0.648	0.549	0.681	0.560	0.726	0.584	0.718	0.580	1.070	0.710	0.685	0.559	0.695	0.569	0.925	0.647
	ETTh2	0.360	0.394	0.380	0.413	0.398	0.426	0.400	0.433	0.437	0.437	0.517	0.472	0.488	0.475	0.462	0.443	0.439	0.448	0.463	0.454
	ETTm1	0.474	0.447	0.455	0.446	0.477	0.451	0.472	0.450	0.657	0.533	0.619	0.521	0.784	0.596	0.526	0.477	0.526	0.476	0.717	0.561
	ETTm2	0.293	0.338	0.296	0.342	0.307	0.348	0.308	0.346	0.324	0.357	0.320	0.355	0.356	0.388	0.311	0.345	0.314	0.352	0.344	0.372
	Average	0.427	0.421	0.445	0.438	0.458	0.444	0.465	0.447	0.605	0.511	0.606	0.509	0.675	0.542	0.496	0.456	0.494	0.461	0.612	0.509
10%	ETTh1	0.543	0.493	0.593	0.529	0.785	0.553	0.590	0.525	0.700	0.568	0.685	0.552	0.910	0.860	0.625	0.532	0.633	0.542	0.869	0.628
	ETTh2	0.372	0.402	0.419	0.439	0.424	0.441	0.397	0.421	0.456	0.446	0.474	0.451	0.489	0.483	0.463	0.443	0.415	0.431	0.479	0.465
	ETTm1	0.465	0.436	0.455	0.435	0.487	0.461	0.464	0.441	0.598	0.502	0.557	0.481	0.728	0.565	0.455	0.439	0.501	0.466	0.677	0.537
	ETTm2	0.279	0.327	0.284	0.332	0.305	0.344	0.293	0.335	0.301	0.336	0.306	0.343	0.336	0.373	0.295	0.330	0.296	0.343	0.320	0.353
	Average	0.415	0.415	0.438	0.434	0.500	0.450	0.436	0.431	0.562	0.478	0.513	0.460	0.616	0.570	0.460	0.436	0.461	0.446	0.586	0.496

Table 4: Zero-shot learning results from a source dataset to an unseen target dataset (e.g., ETTh1 → ETTh2). Detailed results are provided in Appendix E.4.

Methods	**S^{2}TS-LLM (Ours)**		S^2 IP-LLM [7]		Time-LLM [9]		GPT4TS [22]		TimeMixer [41]		TimeXer [38]		iTransformer [39]		RLinear [17]		PatchTST [40]		TimesNet [13]	
Metric	MSE ↓	MAE ↓	MSE ↓	MAE ↓	MSE ↓	MAE ↓	MSE ↓	MAE ↓	MSE ↓	MAE ↓	MSE ↓	MAE ↓	MSE ↓	MAE ↓	MSE ↓	MAE ↓	MSE ↓	MAE ↓	MSE ↓	MAE ↓
ETTh1 → ETTh2	0.341	0.387	0.403	0.417	0.384	0.409	0.406	0.422	0.374	0.397	0.390	0.407	0.457	0.455	0.380	0.401	0.380	0.405	0.421	0.431
ETTh1 → ETTm2	0.294	0.350	0.325	0.360	0.317	0.370	0.325	0.363	0.321	0.362	0.330	0.366	0.360	0.390	0.316	0.356	0.314	0.360	0.327	0.361
ETTh2 → ETTh1	0.550	0.513	0.669	0.560	0.663	0.540	0.757	0.578	0.726	0.579	0.602	0.530	0.868	0.625	0.576	0.511	0.565	0.513	0.865	0.621
ETTh2 → ETTm2	0.292	0.350	0.327	0.363	0.339	0.371	0.335	0.370	0.351	0.388	0.350	0.385	0.335	0.382	0.329	0.371	0.325	0.365	0.342	0.376
ETTm1 → ETTh2	0.389	0.417	0.442	0.439	0.440	0.449	0.433	0.439	0.484	0.466	0.530	0.489	0.455	0.458	0.428	0.431	0.439	0.438	0.457	0.454
ETTm1 → ETTm2	0.268	0.323	0.304	0.347	0.311	0.343	0.313	0.348	0.303	0.340	0.310	0.347	0.319	0.363	0.297	0.330	0.296	0.334	0.322	0.354
ETTm2 → ETTh2	0.372	0.408	0.406	0.429	0.429	0.448	0.435	0.443	0.414	0.429	0.413	0.428	0.432	0.447	0.417	0.428	0.409	0.425	0.435	0.443
ETTm2 → ETTm1	0.496	0.462	0.622	0.532	0.588	0.503	0.769	0.567	0.556	0.481	0.710	0.554	0.706	0.572	0.527	0.474	0.568	0.492	0.769	0.567
Average	0.375	0.401	0.437	0.431	0.434	0.429	0.472	0.441	0.441	0.430	0.454	0.438	0.492	0.462	0.409	0.413	0.412	0.417	0.492	0.451

4.3 Few-Shot Learning

Setups. Given the remarkable few-shot learning capabilities of LLMs [44], we follow the setup in [22] to assess the few-shot performance of our method. We train the model using limited data (only the first 5% or 10% data of train set) and evaluate it on the whole test set.

Results. The brief 5% and 10% few-shot learning results are illustrated in Table 3. Our S^{2}TS-LLM generally outperforms the baselines on different datasets and settings, with the exception of the ETTm1 dataset. A possible reason is that ETTm1 has finer temporal resolution and more complex variations than other datasets. This increases the difficulty for our method to capture sparse spectral patterns from limited data, leading to suboptimal results. However, our S^{2}TS-LLM realizes average MSE reductions of 4.1%, 6.7%, and 8.2% over S2IP-LLM, Time-LLM, and GPT4TS, respectively, under the 5% few-shot setting, and reductions of 5.2%, 17.0%, and 4.8% under the 10% few-shot setting. Compared to conventional models such as RLinear and iTransformer, our S^{2}TS-LLM leverages the generalizability of LLMs and yields relative improvements from 6.4% to 34.8% over two settings. These results highlight the effectiveness of our approach in few-shot learning scenarios.

4.4 Zero-Shot Learning

Setups. Beyond few-shot learning, prior work [8] has shown that LLMs also hold promise as effective zero-shot forecasters. To explore this potential, we investigate the zero-shot capabilities of our S^{2}TS-LLM under a cross-domain adaptation setting, where the model is first trained on a source dataset and then directly applied to an unseen target dataset.

Results. The zero-shot learning results in Table 4 show that our S^{2}TS-LLM remarkably excels over all baselines with 8.3% improvement over second-best RLinear and 13.5% improvement over LLM-based Time-LLM in terms of MSE metric. Experiments in both few-shot and zero-shot settings highlight S^{2}TS-LLM's exceptional performance under data-scarce conditions. We attribute this to our approach's ability to transfer the LLM's linguistic knowledge to time-series reasoning by learning robust priors of temporal and contextual patterns.

4.5 Time Series Classification

Setups. To assess the model's ability in representation learning, we conduct experiments on sequence-level classification using the setup outlined by [13]. We select 10 multivariate datasets from the UEA Time Series Classification Archive [45], covering the spectral recognition, medical diagnosis, and other tasks. All datasets are preprocessed by following [46], where different subsets have different sequence lengths.

Results. As shown in Figure 5, our S^{2}TS-LLM achieves the best performance with an average accuracy of **76.4%**, surpassing the LLM-based GPT4TS (74.0%), CNN-based TimesNet (73.6%), and classical method Rocket (72.5%). It is worth noting that some conventional models achieve competitive performance on forecasting tasks with LLM-based methods, but fail in classification tasks, such as PatchTST (67.4%) and RLinear (67.2%). These observations show that the prior linguistic knowledge of LLMs can help the time series representation learning.

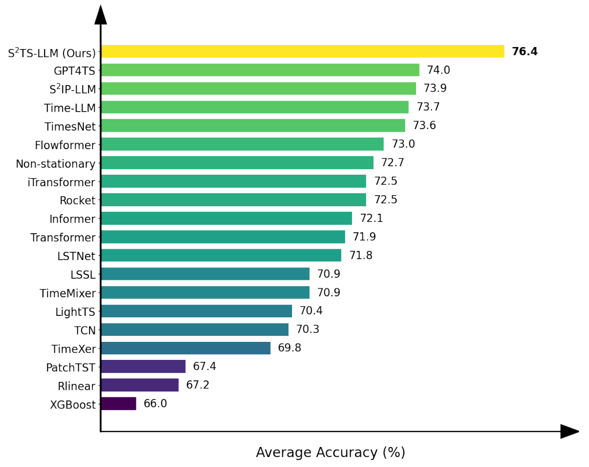

Figure 5: Classification results. The results are averaged from ten datasets of UEA. Detailed results are provided in Appendix E.5.

4.6 Ablation Study

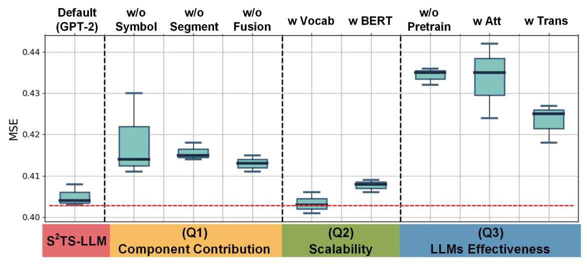

Figure 6: Ablation Study conducted with three experimental repeats. The red dashed line represents the best result of S^{2}TS-LLM. Detailed results are provided in Appendix E.6.

As depicted in Figure 6, we conduct an ablation study with 8 model variants on ETTh1 to evaluate the (Q1) components' contribution to the framework, (Q2) scalability of the framework, and (Q3) LLM effectiveness to time series tasks. To evaluate Q1, the variants **"w/o Symbol"** and **"w/o Segment"** remove the spectral symbolization and contextual segmentation modules, respectively, and **"w/o Fusion"** replaces our fusion strategy with a simple addition of the LLM outputs. These three variants impair the knowledge transfer from language to time series and lead to performance drops, confirming the importance of each designed module. Then, we evaluate Q2 from two aspects: first, **"w Vocab"** replaces ASCII symbols with vocabulary for textual abstracting, but yields similar performance, verifying the scalability of our symbol-based strategy—it effectively captures spectral patterns while avoiding the need for task-specific vocabulary design; second, **"w BERT"** replaces GPT-2 with BERT [47] and still achieves competitive results, demonstrating the framework's scalability across LLM architectures. Regarding Q3, **"w/o Pretrain"** (random LLM initialization), **"w Att"**, and **"w Trans"** (replace the LLM with a single Attention or Transformer layer) all underperform compared to S^{2}TS-LLM, highlighting the value of pre-trained LLMs in time series analysis.

4.7 Visual Interpretation

Interpretation of Spectral Symbolization. We provide a case study on ETTh1 to show the effectiveness of spectral symbolization in Figure 7. The top 4 subplots depict the progressive refinement of spectral symbolization, as the generated textual abstractions (green dots) transition from **(a)** a scattered, random distribution to **(d)** a compact distribution that fits the time series space (blue dots). Figure 7 **(e)** visualizes the cosine similarity between textual abstractions and time series in a heatmap form. We observe that most cosine similarity values are close to 1 (indicated by light green), suggesting that the spectral symbolization effectively generates textual abstractions to capture temporal patterns.

Interpretation of Contextual Segmentation. Figure 8 presents a case study on ETTh2 to illustrate how contextual segmentation divides a temporal sequence into different blocks. We observe that a time series composed of Q patches is generally divided into three main parts: (1) the initial patches are grouped together as the first segment, as they are farthest from the prediction sequence and capture long-range dependencies; (2) the middle patches are segmented based on their varying trends and patterns; and (3) the final patches, which are closest to the prediction sequence, are separated into a distinct segment to model short-range dependencies.

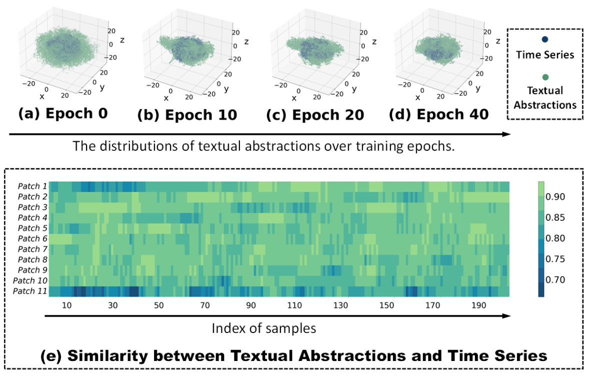

Figure 7: A showcase of spectral symbolization.

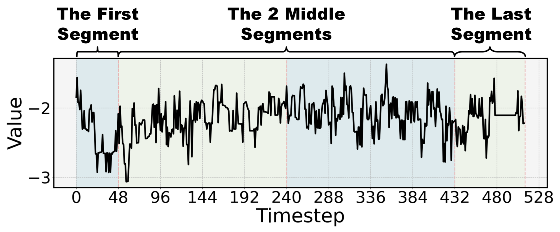

Figure 8: A showcase of contextual segmentation, where different segments distinguished by blue and green colors can be grouped into three main parts.

5 Conclusion

Considering the significant importance of LLMs in complex real-world time series analysis, we empower LLMs' ability to perceive temporal variations and contextual structures. Technically, we revisit the alignment between natural language and time series representations by operating in the frequency domain rather than the time domain, allowing the use of compact symbolic forms to capture frequency semantics. Furthermore, we mitigate contextual discrepancies between time series and language by adapting the LLM's positional indices to reflect segment-level temporal structures. Experimental results show that the proposed S^{2}TS-LLM effectively bridges time series and linguistics, enabling LLMs to generalize across diverse time-series tasks while achieving promising performance.

6 Acknowledgment

This work is supported in part by the National Key-Research and Development Program of China (Grant No. 2020YFB2104003), the Natural Science Foundation of China (Grant Nos. 62402168, U23A20322), and the Natural Science Foundation of Hunan Province (Grant No. 2024JJ6156).

References

[1] Q. S. Wen, L. X. Yang, T. Zhou, and L. Sun. Robust time series analysis and applications: An industrial perspective. In *Proceedings of ACM SIGKDD Conference on Knowledge Discovery and Data Mining*, pages 4836–4837, 2022.

[2] G. K. Lai, W. C. Chang, Y. M Yang, and H. X. Liu. Modeling long-and short-term temporal patterns with deep neural networks. In *Proceedings of International ACM SIGIR Conference on Research Development in Information Retrieval*, pages 95–104, 2018.

[3] H. X. Wu, J. H. Xu, J. M. Wang, and M. S. Long. Autoformer: Decomposition transformers with auto-correlation for long-term series forecasting. In *Advances in Neural Information Processing Systems*, pages 22419–22430, 2021.

[4] A. L. Zeng, M. X. Chen, L. Zhang, and Q. Xu. Are transformers effective for time series forecasting? In *Proceedings of AAAI Conference on Artificial Intelligence*, pages 11121–11128, 2023.

[5] P. Y. Liu, H. Guo, T. Dai, N. Q. Li, J. G. Bao, X. D. Ren, Y. Jiang, and S. T. Xia. Calf: Aligning llms for time series forecasting via cross-modal fine-tuning. In *Proceedings of AAAI Conference on Artificial Intelligence*, pages 18915–18923, 2025.

[6] H. X. Liu, H. Kamarthi, Z. Y. Zhao, S. Q. Xu, S. Y. Wang, Q. S. Wen, T. Hartvigsen, F. Wang, and B. Prakash. How can time series analysis benefit from multiple modalities? a survey and outlook. *arXiv preprint arXiv:2503.11835*, 2025.

[7] Z. J. Pan, Y. S. Jiang, S. Garg, A. Schneider, Y. Nevmyvaka, and D. J. Song. s^2ip-llm: Semantic space informed prompt learning with llm for time series forecasting. In *Proceedings of International Conference on Machine Learning*, pages 1–19, 2024.

[8] N. Gruver, M. Finzi, S. K. Qiu, and A. G. Wilson. Large language models are zero-shot time series forecasters. In *Advances in Neural Information Processing Systems*, pages 19622–19635, 2023.

[9] M. Jin, S. Y. Wang, L. T. Ma, Z. X. Chu, J. Y. Zhang, X. M. Shi, P. Y Chen, Y. X. Liang, Y. F. Li, S. R. Pan, and Q. S. Wen. Time-llm: Time series forecasting by reprogramming large language models. In *Proceedings of International Conference on Learning Representations*, pages 1–24, 2024.

[10] H. J. Nussbaumer. *The fast Fourier transform.* Springer Berlin Heidelberg, 1982.

[11] E. C. Nie, S. Z. Yuan, B. L. Ma, H. Schmid, M. Färber, F. Kreuter, and H. Schütze. Decomposed prompting: Unveiling multilingual linguistic structure knowledge in english-centric large language models. *arXiv preprint arXiv:2402.18397*, 2024.

[12] L. A Wang, L. Li, D. M. Dai, D. L. Chen, H. Zhou, F. D. Meng, J. Zhou, , and X. Sun. Label words are anchors: An information flow perspective for understanding in-context learning. In *Proceedings of Empirical Methods in Natural Language Processing*, page 9840–9855, 2023.

[13] H. X. Wu, T. G. Hu, Y. Liu, H. Zhou, J. M Wang, and M. S. Long. Timesnet: Temporal 2d-variation modeling for general time series analysis. In *Proceedings of International Conference on Learning Representations*, pages 1–23, 2023.

[14] Z. L. Jiang, Z. F. Ning, H. Miao, and L. Wang. Stdnet: A spatio-temporal decomposition neural network for multivariate time series forecasting. *Tsinghua Science and Technology*, 29(4):1232–1247, 2024.

[15] S. Vasantha Kumar and L. Vanajakshi. Short-term traffic flow prediction using seasonal arima model with limited input data. *European Transport Research Review*, 7(3):1–9, 2015.

[16] T. Zhou, Z. Q. Ma, X. Wang, Q. S. Wen, L. Sun, T. Yao, W. T. Yin, and R. Jin. Film: Frequency improved legendre memory model for long-term time series forecasting. In *Advances in Neural Information Processing Systems*, pages 12677–12690, 2022.

[17] Z. Li, S. Y. Qi, Y. D. Li, and Z. L. Xu. Revisiting long-term time series forecasting: An investigation on linear mapping. *arXiv preprint arXiv:2305.10721*, 2023.

[18] T. Zhou, Q. S. Wen Z. Q. Ma, X. Wang, L. Sun, and R. Jin. Fedformer: Frequency enhanced decomposed transformer for long-term series forecasting. In *Proceedings of International Conference on Machine Learning*, pages 27268–27286, 2022.

[19] W. Z. Yue, Y. Liu, X. H. Ying, B. W. Xing, R. H. Guo, and J. Shi. Freeformer: Frequency enhanced transformer for multivariate time series forecasting. *arXiv preprint arXiv:2501.13989*, 2025.

[20] M. Jin, Y. F. Zhang, W. Chen, K. X. Zhang, Y. X. Liang, B. Yang, J. D. Wang, S. R. Pan, and Q. S. Wen. Position: What can large language models tell us about time series analysis. In *Proceedings of International Conference on Machine Learning*, pages 1–17, 2024.

[21] C. M. Yeh, X. Dai, H. Y. Chen, Y. Zheng, Y. J. Fan, A. Der, V. Lai, Z. F. Zhuang, J. P. Wang, L. Wang, and W. Zhang. Toward a foundation model for time series data. In *Proceedings of ACM International Conference on Information Knowledge Management*, pages 4400–4404, 2023.

[22] T. Zhou, P. S. Niu, X. Wang, L. Sun, and R. Jin. One fits all: Power general time series analysis by pretrained lm. In *Advances in Neural Information Processing Systems*, pages 43322–43355, 2023.

[23] C. Chang, W. Y. Wang, W. C. Peng, and T. F. Chen. Llm4ts: Aligning pre-trained llms as data-efficient time-series forecasters. *ACM Transactions on Intelligent Systems and Technology*, 16(3):1–20, 2025.

[24] X. L. Zhang, S. Y. Li, Z. Y. Chen, X. F. Yan, and L. R. Petzold. Improving medical predictions by irregular multimodal electronic health records modeling. In *Proceedings of International Conference on Machine Learning*, pages 41300–41313, 2023.

[25] Y. Liu, X. D. Huang G. Qin, J. M. Wang, and M. S. Long. Autotimes: Autoregressive time series forecasters via large language models. In *Advances in Neural Information Processing Systems*, pages 122154–122184, 2024.

[26] C. X. Liu, Q. X. Xu, H. Miao, S. Yang, L. Z. Zhang, C. Long, Z. Y. Li, and R. Zhao. Timecma: Towards llm-empowered multivariate time series forecasting via cross-modality alignment. In *Proceedings of AAAI Conference on Artificial Intelligence*, pages 18780–18788, 2025.

[27] Y. X. Hu, Q. Li, D. X. Zhang, J. Y. Yan, and Y. T. Chen. Context-alignment: Activating and enhancing llm capabilities in time series. In *Proceedings of International Conference on Learning Representations*, pages 1–20, 2025.

[28] D. F. Cao, F. R. Jia, S. O. Arik, T. Pfister, Y. X. Zheng, W. Ye, and Y. Liu. Tempo: Prompt-based generative pre-trained transformer for time series forecasting. In *Proceedings of International Conference on Learning Representations*, pages 1–33, 2024.

[29] C. X. Sun, H. Y. Li, Y. L. Li, and S. D. Hong. Test: Text prototype aligned embedding to activate llm's ability for time series. In *Proceedings of International Conference on Learning Representations*, pages 1–25, 2024.

[30] C. Chatfield. *The analysis of time series: an introduction*. Chapman and hall/CRC, 1981.

[31] R. Liu, E. L. Zippi, H. Pouransari, C. Sandino, J. P Nie, H. Goh, E. Azemi, and A. Moin. Frequency-aware masked autoencoders for multimodal pretraining on biosignals. *arXiv preprint arXiv:2402.18397*, 2024.

[32] X. Zhang, Z. Y. Zhao, T. Tsiligkaridis, and M. Zitnik. Self-supervised contrastive pre-training for time series via time-frequency consistency. In *Advances in Neural Information Processing Systems*, pages 3988–4003, 2022.

[33] W. J. Su. Do large language models (really) need statistical foundations? *arXiv preprint arXiv:2505.19145*, 2025.

[34] G. X. Chen, H. Shi, J. W. Li, Y. H. Gao, X. Z. Ren, Y. M. Chen, X. Jiang, Z. G. Li, W. Y. Liu, and C. Huang. Sepllm: Accelerate large language models by compressing one segment into one separator. In *Proceedings of International Conference on Machine Learning*, pages 1–21, 2025.

[35] F. Q. Jiang, Z. C. Xu, L. Y Niu, Z. Xiang, B. Ramasubramanian, B. Li, and R. Poovendran. Artprompt: Ascii art-based jailbreak attacks against aligned llms. In *Proceedings of Annual Meeting of the Association for Computational Linguistics*, pages 15157–15173, 2024.

[36] H. Xue and F. D. Salim. Promptcast: A new prompt-based learning paradigm for time series forecasting. *IEEE Transactions on Knowledge and Data Engineering*, 36(11):6851–6864, 2023.

[37] M. Beck, K. Pöppel, M. Spanring, A. Auer, O. Prudnikova, M. Kopp, G. Klambauer, J. Brandstetter, and S. Hochreiter. xlstm: Extended long short-term memory. In *Advances in Neural Information Processing Systems*, pages 107547–107603, 2024.

[38] Y. X. Wang, H. X. Wu, J. X. Dong, G. Qin, H. R. Zhang, Y. Liu, Y. Z. Qiu, J. M. Wang, and M. S. Long. Timexer: Empowering transformers for time series forecasting with exogenous variables. In *Advances in Neural Information Processing Systems*, pages 1–30, 2024.

[39] Y. Liu, T. G. Hu, H. R. Zhang, H. X. Wu, S. Wang, L. T. Ma, and M. S. Long. itransformer: Inverted transformers are effective for time series forecasting. In *Proceedings of International Conference on Learning Representations*, pages 1–25, 2023.

[40] Y. Q. Nie, N. H. Nguyen, P. Sinthong, and J. Kalagnanam. A time series is worth 64 words: Long-term forecasting with transformers. In *Proceedings of International Conference on Learning Representations*, pages 1–24, 2023.

[41] S. Y. Wang, H. X. Wu, X. M. Shi, T. G. Hu, H. K. Luo, L. T. Ma, J. Y. Zhang, and J. Zhou. Timemixer: Decomposable multiscale mixing for time series forecasting. In *Proceedings of International Conference on Learning Representations*, pages 1–27, 2024.

[42] A. Radford, J. Wu, R. Child, D. Luan, D. Amodei, and I. Sutskever. Language models are unsupervised multitask learners. *OpenAI blog*, 1(8):1–24, 2019.

[43] Spyros Makridakis and Michele Hibon. The m3-competition: results, conclusions and implications. *International Journal of Forecasting*, 16(4):451–476, 2000.

[44] X. Liu, D. McDuff, G. Kovacs, I. Galatzer-Levy, J. Sunshine, J. N. Zhan, M. Z. Poh, S. Liao, P. D. Achille, and S. Patel. Large language models are few-shot health learners. *arXiv preprint arXiv:2305.15525*, 2023.

[45] A. J. Bagnall, H. A. Dau, J. Lines, M. Flynn, J. Large, A. G. Bostrom, P. Southam, and E. J. Keogh. The uea multivariate time series classification archive. *arXiv preprint arXiv:1811.00075*, 2018.

[46] G. Zerveas, S. Jayaraman, D. Patel, A. Bhamidipaty, and C. Eickhoff. A transformer-based framework for multivariate time series representation learning. In *Proceedings of ACM SIGKDD Conference on Knowledge Discovery and Data Mining*, pages 2114–2124, 2021.

[47] J. Devlin, M. W. Chang, K. Lee, , and K. Toutanova. Bert: pre-training of deep bidirectional transformers for language understanding. *CoRR, abs/1810.04805*, 2018.

[48] Y. Liu, H. X. Wu, J. M Wang, and M. S. Long. Non-stationary transformers: Exploring the stationarity in time series forecasting. In *Advances in Neural Information Processing Systems*, pages 9881–9893, 2022.

[49] Z. Y. Huang, X. Y. Shi, C. Zhang, Q. Wang, K. C. Cheung, H. W. Qin, J. F. Dai, and H. S. Li. Flowformer: A transformer architecture for optical flow. In *Proceedings of European Conference on Computer Vision*, pages 668–685, 2022.

[50] H. Y. Zhou, S. H. Zhang, J. Q. Peng, S. Zhang, J. X. Li, H. Xiong, and W. C. Zhang. Informer: Beyond efficient transformer for long sequence time-series forecasting. In *Proceedings of AAAI Conference on Artificial Intelligence*, pages 11106–11115, 2021.

[51] A. Vaswani, N. Shazeer, and N. Parmar. Attention is all you need. In *Advances in Neural Information Processing Systems*, pages 6000–6010, 2017.

[52] T. Zhang, Y. Zhang, W. Cao, J. Bian, X. Yi, S. Zheng, , and J. Li. Less is more: Fast multivariate time series forecasting with light sampling-oriented mlp structures. *arXiv preprint arXiv:2207.01186*, 2022.

[53] J. Y. Franceschi, A. Dieuleveut, and M. Jaggi. Unsupervised scalable representation learning for multivariate time series. In *Advances in Neural Information Processing Systems*, page 32, 2019.

[54] A. Gu, K. Goel, and C. Ré. Efficiently modeling long sequences with structured state spaces. *arXiv preprint arXiv:2111.00396*, 2021.

[55] A. Dempster, F. Petitjean, and G. I. Webb. Rocket: exceptionally fast and accurate time series classification using random convolutional kernels. *Data Mining and Knowledge Discovery*, 34(5):1454–1495, 2020.

[56] T. Q. Chen and C. Guestrin. Xgboost: A scalable tree boosting system. In *Proceedings of ACM SIGKDD Conference on Knowledge Discovery and Data Mining*, pages 785–794, 2016.

NeurIPS Paper Checklist

1. **Claims**

   Question: Do the main claims made in the abstract and introduction accurately reflect the paper's contributions and scope?

   Answer: [Yes]

   Justification: The abstract and Section 1 have claimed the contributions made in the paper.

   Guidelines:

   - The answer NA means that the abstract and introduction do not include the claims made in the paper.
   - The abstract and/or introduction should clearly state the claims made, including the contributions made in the paper and important assumptions and limitations. A No or NA answer to this question will not be perceived well by the reviewers.
   - The claims made should match theoretical and experimental results, and reflect how much the results can be expected to generalize to other settings.
   - It is fine to include aspirational goals as motivation as long as it is clear that these goals are not attained by the paper.

2. **Limitations**

   Question: Does the paper discuss the limitations of the work performed by the authors?

   Answer: [Yes]

   Justification: Please refer to the discussion section in Appendix D.

   Guidelines:

   - The answer NA means that the paper has no limitation while the answer No means that the paper has limitations, but those are not discussed in the paper.
   - The authors are encouraged to create a separate "Limitations" section in their paper.
   - The paper should point out any strong assumptions and how robust the results are to violations of these assumptions (e.g., independence assumptions, noiseless settings, model well-specification, asymptotic approximations only holding locally). The authors should reflect on how these assumptions might be violated in practice and what the implications would be.
   - The authors should reflect on the scope of the claims made, e.g., if the approach was only tested on a few datasets or with a few runs. In general, empirical results often depend on implicit assumptions, which should be articulated.
   - The authors should reflect on the factors that influence the performance of the approach. For example, a facial recognition algorithm may perform poorly when image resolution is low or images are taken in low lighting. Or a speech-to-text system might not be used reliably to provide closed captions for online lectures because it fails to handle technical jargon.
   - The authors should discuss the computational efficiency of the proposed algorithms and how they scale with dataset size.
   - If applicable, the authors should discuss possible limitations of their approach to address problems of privacy and fairness.
   - While the authors might fear that complete honesty about limitations might be used by reviewers as grounds for rejection, a worse outcome might be that reviewers discover limitations that aren't acknowledged in the paper. The authors should use their best judgment and recognize that individual actions in favor of transparency play an important role in developing norms that preserve the integrity of the community. Reviewers will be specifically instructed to not penalize honesty concerning limitations.

3. **Theory assumptions and proofs**

   Question: For each theoretical result, does the paper provide the full set of assumptions and a complete (and correct) proof?

   Answer: [NA]

Justification: This paper does not include theoretical results.

Guidelines:

- The answer NA means that the paper does not include theoretical results.
- All the theorems, formulas, and proofs in the paper should be numbered and cross-referenced.
- All assumptions should be clearly stated or referenced in the statement of any theorems.
- The proofs can either appear in the main paper or the supplemental material, but if they appear in the supplemental material, the authors are encouraged to provide a short proof sketch to provide intuition.
- Inversely, any informal proof provided in the core of the paper should be complemented by formal proofs provided in appendix or supplemental material.
- Theorems and Lemmas that the proof relies upon should be properly referenced.

4. **Experimental result reproducibility**

   Question: Does the paper fully disclose all the information needed to reproduce the main experimental results of the paper to the extent that it affects the main claims and/or conclusions of the paper (regardless of whether the code and data are provided or not)?

   Answer: [Yes]

   Justification: The framework design has been fully described in the Section 3 and the training details are provided in Appendix B.3.

   Guidelines:

   - The answer NA means that the paper does not include experiments.
   - If the paper includes experiments, a No answer to this question will not be perceived well by the reviewers: Making the paper reproducible is important, regardless of whether the code and data are provided or not.
   - If the contribution is a dataset and/or model, the authors should describe the steps taken to make their results reproducible or verifiable.
   - Depending on the contribution, reproducibility can be accomplished in various ways. For example, if the contribution is a novel architecture, describing the architecture fully might suffice, or if the contribution is a specific model and empirical evaluation, it may be necessary to either make it possible for others to replicate the model with the same dataset, or provide access to the model. In general. releasing code and data is often one good way to accomplish this, but reproducibility can also be provided via detailed instructions for how to replicate the results, access to a hosted model (e.g., in the case of a large language model), releasing of a model checkpoint, or other means that are appropriate to the research performed.
   - While NeurIPS does not require releasing code, the conference does require all submissions to provide some reasonable avenue for reproducibility, which may depend on the nature of the contribution. For example
     (a) If the contribution is primarily a new algorithm, the paper should make it clear how to reproduce that algorithm.
     (b) If the contribution is primarily a new model architecture, the paper should describe the architecture clearly and fully.
     (c) If the contribution is a new model (e.g., a large language model), then there should either be a way to access this model for reproducing the results or a way to reproduce the model (e.g., with an open-source dataset or instructions for how to construct the dataset).
     (d) We recognize that reproducibility may be tricky in some cases, in which case authors are welcome to describe the particular way they provide for reproducibility. In the case of closed-source models, it may be that access to the model is limited in some way (e.g., to registered users), but it should be possible for other researchers to have some path to reproducing or verifying the results.

5. **Open access to data and code**

   Question: Does the paper provide open access to the data and code, with sufficient instructions to faithfully reproduce the main experimental results, as described in supplemental material?

Answer: [Yes]

Justification: Please refer to the dataset details listed in Appendix B.1. The key code can be found in the supplementary materials, and the full code will be published if the paper is accepted.

Guidelines:

- The answer NA means that paper does not include experiments requiring code.
- Please see the NeurIPS code and data submission guidelines (`https://nips.cc/public/guides/CodeSubmissionPolicy`) for more details.
- While we encourage the release of code and data, we understand that this might not be possible, so "No" is an acceptable answer. Papers cannot be rejected simply for not including code, unless this is central to the contribution (e.g., for a new open-source benchmark).
- The instructions should contain the exact command and environment needed to run to reproduce the results. See the NeurIPS code and data submission guidelines (`https://nips.cc/public/guides/CodeSubmissionPolicy`) for more details.
- The authors should provide instructions on data access and preparation, including how to access the raw data, preprocessed data, intermediate data, and generated data, etc.
- The authors should provide scripts to reproduce all experimental results for the new proposed method and baselines. If only a subset of experiments are reproducible, they should state which ones are omitted from the script and why.
- At submission time, to preserve anonymity, the authors should release anonymized versions (if applicable).
- Providing as much information as possible in supplemental material (appended to the paper) is recommended, but including URLs to data and code is permitted.

6. **Experimental setting/details**

   Question: Does the paper specify all the training and test details (e.g., data splits, hyper-parameters, how they were chosen, type of optimizer, etc.) necessary to understand the results?

   Answer: [Yes]

   Justification: Please refer to Appendix B.

   Guidelines:

   - The answer NA means that the paper does not include experiments.
   - The experimental setting should be presented in the core of the paper to a level of detail that is necessary to appreciate the results and make sense of them.
   - The full details can be provided either with the code, in appendix, or as supplemental material.

7. **Experiment statistical significance**

   Question: Does the paper report error bars suitably and correctly defined or other appropriate information about the statistical significance of the experiments?

   Answer: [Yes]

   Justification: Please refer to the results in subsection 4.6 and Appendix E.6.

   Guidelines:

   - The answer NA means that the paper does not include experiments.
   - The authors should answer "Yes" if the results are accompanied by error bars, confidence intervals, or statistical significance tests, at least for the experiments that support the main claims of the paper.
   - The factors of variability that the error bars are capturing should be clearly stated (for example, train/test split, initialization, random drawing of some parameter, or overall run with given experimental conditions).
   - The method for calculating the error bars should be explained (closed form formula, call to a library function, bootstrap, etc.)
   - The assumptions made should be given (e.g., Normally distributed errors).

- It should be clear whether the error bar is the standard deviation or the standard error of the mean.
- It is OK to report 1-sigma error bars, but one should state it. The authors should preferably report a 2-sigma error bar than state that they have a 96% CI, if the hypothesis of Normality of errors is not verified.
- For asymmetric distributions, the authors should be careful not to show in tables or figures symmetric error bars that would yield results that are out of range (e.g. negative error rates).
- If error bars are reported in tables or plots, The authors should explain in the text how they were calculated and reference the corresponding figures or tables in the text.

8. **Experiments compute resources**

   Question: For each experiment, does the paper provide sufficient information on the computer resources (type of compute workers, memory, time of execution) needed to reproduce the experiments?

   Answer: [Yes]

   Justification: Please refer to Appendix B.3.

   Guidelines:

   - The answer NA means that the paper does not include experiments.
   - The paper should indicate the type of compute workers CPU or GPU, internal cluster, or cloud provider, including relevant memory and storage.
   - The paper should provide the amount of compute required for each of the individual experimental runs as well as estimate the total compute.
   - The paper should disclose whether the full research project required more compute than the experiments reported in the paper (e.g., preliminary or failed experiments that didn't make it into the paper).

9. **Code of ethics**

   Question: Does the research conducted in the paper conform, in every respect, with the NeurIPS Code of Ethics `https://neurips.cc/public/EthicsGuidelines`?

   Answer: [Yes]

   Justification: We have reviewed and the reasearch conforms with the NeurIPS Code of Ethics.

   Guidelines:

   - The answer NA means that the authors have not reviewed the NeurIPS Code of Ethics.
   - If the authors answer No, they should explain the special circumstances that require a deviation from the Code of Ethics.
   - The authors should make sure to preserve anonymity (e.g., if there is a special consideration due to laws or regulations in their jurisdiction).

10. **Broader impacts**

    Question: Does the paper discuss both potential positive societal impacts and negative societal impacts of the work performed?

    Answer: [Yes]

    Justification: Please refer to the discussion section in Appendix D.

    Guidelines:

    - The answer NA means that there is no societal impact of the work performed.
    - If the authors answer NA or No, they should explain why their work has no societal impact or why the paper does not address societal impact.
    - Examples of negative societal impacts include potential malicious or unintended uses (e.g., disinformation, generating fake profiles, surveillance), fairness considerations (e.g., deployment of technologies that could make decisions that unfairly impact specific groups), privacy considerations, and security considerations.

- The conference expects that many papers will be foundational research and not tied to particular applications, let alone deployments. However, if there is a direct path to any negative applications, the authors should point it out. For example, it is legitimate to point out that an improvement in the quality of generative models could be used to generate deepfakes for disinformation. On the other hand, it is not needed to point out that a generic algorithm for optimizing neural networks could enable people to train models that generate Deepfakes faster.
- The authors should consider possible harms that could arise when the technology is being used as intended and functioning correctly, harms that could arise when the technology is being used as intended but gives incorrect results, and harms following from (intentional or unintentional) misuse of the technology.
- If there are negative societal impacts, the authors could also discuss possible mitigation strategies (e.g., gated release of models, providing defenses in addition to attacks, mechanisms for monitoring misuse, mechanisms to monitor how a system learns from feedback over time, improving the efficiency and accessibility of ML).

11. **Safeguards**

    Question: Does the paper describe safeguards that have been put in place for responsible release of data or models that have a high risk for misuse (e.g., pre-trained language models, image generators, or scraped datasets)?

    Answer: [NA]

    Justification: The paper does not pose no such risks.

    Guidelines:

    - The answer NA means that the paper poses no such risks.
    - Released models that have a high risk for misuse or dual-use should be released with necessary safeguards to allow for controlled use of the model, for example by requiring that users adhere to usage guidelines or restrictions to access the model or implementing safety filters.
    - Datasets that have been scraped from the Internet could pose safety risks. The authors should describe how they avoided releasing unsafe images.
    - We recognize that providing effective safeguards is challenging, and many papers do not require this, but we encourage authors to take this into account and make a best faith effort.

12. **Licenses for existing assets**

    Question: Are the creators or original owners of assets (e.g., code, data, models), used in the paper, properly credited and are the license and terms of use explicitly mentioned and properly respected?

    Answer: [Yes]

    Justification: All creators of datasets are properly credited by citations.

    Guidelines:

    - The answer NA means that the paper does not use existing assets.
    - The authors should cite the original paper that produced the code package or dataset.
    - The authors should state which version of the asset is used and, if possible, include a URL.
    - The name of the license (e.g., CC-BY 4.0) should be included for each asset.
    - For scraped data from a particular source (e.g., website), the copyright and terms of service of that source should be provided.
    - If assets are released, the license, copyright information, and terms of use in the package should be provided. For popular datasets, `paperswithcode.com/datasets` has curated licenses for some datasets. Their licensing guide can help determine the license of a dataset.
    - For existing datasets that are re-packaged, both the original license and the license of the derived asset (if it has changed) should be provided.

- If this information is not available online, the authors are encouraged to reach out to the asset's creators.

13. **New assets**

    Question: Are new assets introduced in the paper well documented and is the documentation provided alongside the assets?

    Answer: [NA]

    Justification: The paper does not release new assets.

    Guidelines:

    - The answer NA means that the paper does not release new assets.
    - Researchers should communicate the details of the dataset/code/model as part of their submissions via structured templates. This includes details about training, license, limitations, etc.
    - The paper should discuss whether and how consent was obtained from people whose asset is used.
    - At submission time, remember to anonymize your assets (if applicable). You can either create an anonymized URL or include an anonymized zip file.

14. **Crowdsourcing and research with human subjects**

    Question: For crowdsourcing experiments and research with human subjects, does the paper include the full text of instructions given to participants and screenshots, if applicable, as well as details about compensation (if any)?

    Answer: [NA]

    Justification: The paper does not involve crowdsourcing nor research with human subjects.

    Guidelines:

    - The answer NA means that the paper does not involve crowdsourcing nor research with human subjects.
    - Including this information in the supplemental material is fine, but if the main contribution of the paper involves human subjects, then as much detail as possible should be included in the main paper.
    - According to the NeurIPS Code of Ethics, workers involved in data collection, curation, or other labor should be paid at least the minimum wage in the country of the data collector.

15. **Institutional review board (IRB) approvals or equivalent for research with human subjects**

    Question: Does the paper describe potential risks incurred by study participants, whether such risks were disclosed to the subjects, and whether Institutional Review Board (IRB) approvals (or an equivalent approval/review based on the requirements of your country or institution) were obtained?

    Answer: [NA]

    Justification: The paper does not involve crowdsourcing nor research with human subjects.

    Guidelines:

    - The answer NA means that the paper does not involve crowdsourcing nor research with human subjects.
    - Depending on the country in which research is conducted, IRB approval (or equivalent) may be required for any human subjects research. If you obtained IRB approval, you should clearly state this in the paper.
    - We recognize that the procedures for this may vary significantly between institutions and locations, and we expect authors to adhere to the NeurIPS Code of Ethics and the guidelines for their institution.
    - For initial submissions, do not include any information that would break anonymity (if applicable), such as the institution conducting the review.

16. **Declaration of LLM usage**

Question: Does the paper describe the usage of LLMs if it is an important, original, or non-standard component of the core methods in this research? Note that if the LLM is used only for writing, editing, or formatting purposes and does not impact the core methodology, scientific rigorousness, or originality of the research, declaration is not required.

Answer: [Yes]

Justification: The paper provides a detailed description of the use of GPT-2 as a backbone model in the main text.

Guidelines:

- The answer NA means that the core method development in this research does not involve LLMs as any important, original, or non-standard components.
- Please refer to our LLM policy (`https://neurips.cc/Conferences/2025/LLM`) for what should or should not be described.

A Notations

The main notations used in this paper are described in Table 5.

Table 5: A summary of notations.

Symbol	Description
$\boldsymbol{X}, \hat{\boldsymbol{X}}$	Raw and patched time series
$\boldsymbol{Y}, \hat{\boldsymbol{Y}}$	Ground truth and prediction
$\boldsymbol{T}$	Textual Abstractions of time series
$\boldsymbol{P}$	Positional index of the LLMs
f	frequency
v	textual token
$\boldsymbol{c}$	Hidden embeddings of GRU
$\boldsymbol{s}$	segment score
$\boldsymbol{E}$	Embeddings of time series or textual abstractions
$\boldsymbol{H}$	Task-specific prompts
$\boldsymbol{\tau}$	Learnable timestamp parameter
$\boldsymbol{Z}$	Inputs of the LLMs
$\boldsymbol{O}$	Outputs of the LLMs
$\boldsymbol{A}$	Cosine similarity between time series and textual abastractions
L	Length of input time series
N	Number of variants
Q	Number of patches
M	Patch size
R	Stride
B	Number of segments

B Implementation

B.1 Dataset Descriptions

We conduct experiments on 23 real-world datasets to evaluate the performance of our proposed S^{2}TS-LLM. These datasets span domains such as energy, weather, transportation, finance, and healthcare, and have been widely used as benchmarks for time series analysis tasks, including forecasting and classification. Dataset statistics are summarized in Table 6.

Regarding the long-term forecasting task, we utilize 7 well-acknowledged multivariate datasets, including: (1) **Weather** comprises 21 meteorological variables collected at 10-minute intervals by the Weather Station of the Max Planck Biogeochemistry Institute in 2020. (2) **Electricity (ECL)** provides hourly measurements of electricity consumption from 321 consumers. (3) **Traffic** contains hourly road occupancy rates collected from 862 sensors installed along the San Francisco Bay Area freeways. (4) **Electricity Transformer Temperature (ETT)** is a key indicator reflecting long-term electric power usage. The dataset provides six power load features and one target variable, the 'oil temperature', collected over two years from two countries in China. It is divided into 4 distinct subsets where ETTh1 and ETTh2 contain hourly recordings, and ETTm1 and ETTm2 are sampled every 15 minutes. We note that the ETTh1, ETTh2, ETTm1, and ETTm2 datasets are additionally employed for few-shot and zero-shot learning.

Regarding the short-term forecasting task, we adopt the M4 benchmark for performance evaluation. The M4 dataset consists of 100,000 time series from diverse domains, including business, finance, and economics. These time series data are grouped into six distinct subsets with sampling rates ranging from yearly to hourly.

Regarding the time series classification task, we conduct experiments on the UEA Multivariate Time Series Classification Archive [45], which comprises 30 sub-datasets of time series gathered from diverse fields. Following [13], we select 10 multivariate subsets from the UEA archive for classification tasks, covering gesture, action, and audio recognition, medical diagnosis, and other practical tasks.

Table 6: Dataset specifications across different tasks. Notably, the few-shot and zero-shot learning tasks utilize the same datasets as long-term forecasting, but only sample the first 5% or 10% of the data for training.

Tasks	Dataset	Dim	Series Length	Dataset Size	Information (Frequency)
Long-term Forecasting	ETTm1, ETTm2	7	{96, 192, 336, 720}	(34465, 11521, 11521)	Electricity (15 mins)
	ETTh1, ETTh2	7	{96, 192, 336, 720}	(8545, 2881, 2881)	Electricity (Hourly)
	Electricity	321	{96, 192, 336, 720}	(18317, 2633, 5261)	Electricity (Hourly)
	Traffic	862	{96, 192, 336, 720}	(12185, 1757, 3509)	Transportation (Hourly)
	Weather	21	{96, 192, 336, 720}	(36792, 5271, 10540)	Weather (10 mins)
Short-term Forecasting	M4-Yearly	1	6	(23000, 0, 23000)	Demographic
	M4-Quarterly	1	8	(24000, 0, 24000)	Finance
	M4-Monthly	1	18	(48000, 0, 48000)	Industry
	M4-Weekly	1	13	(359, 0, 359)	Macro
	M4-Daily	1	14	(4227, 0, 4227)	Micro
	M4-Hourly	1	48	(414, 0, 414)	Other
Classification (UEA)	EthanolConcentration	3	1751	(261, 0, 263)	Alcohol Industry
	FaceDetection	144	62	(5890, 0, 3524)	Face (250Hz)
	Handwriting	3	152	(150, 0, 850)	Handwriting
	Heartbeat	61	405	(204, 0, 205)	Heart Beat
	JapaneseVowels	12	29	(270, 0, 370)	Voice
	PEMS-SF	963	144	(267, 0, 173)	Transportation (Daily)
	SelfRegulationSCP1	6	896	(268, 0, 293)	Health (256Hz)
	SelfRegulationSCP2	7	1152	(200, 0, 180)	Health (256Hz)
	SpokenArabicDigits	13	93	(6599, 0, 2199)	Voice (11025Hz)
	UWaveGestureLibrary	3	315	(120, 0, 320)	Gesture

B.2 Baselines

We compare our S^{2}TS-LLM against a series of well-known and advanced baselines for forecasting tasks, including LLM-based models (S^{2}IP-LLM [7], Time-LLM [9], GPT4TS [22]), Transformer-based models (TimeXer [38], iTransformer [39], PatchTST [40]), MLP-based models (TimeMixer [41], RLinear [17]), and a CNN-based model (TimesNet [13]). The details of the baselines are shown below.

- S^{2}IP-LLM [7]: S^{2}IP-LLM activates the LLMs for time series tasks by aligning the pre-trained semantic space with time series representation space. Technically, it encodes the large and dense word token embeddings into a small set of semantic anchors and then retrieves the top-k anchors that best match the decomposed time series embeddings, using them as prompts to bootstrap the LLMs' understanding of time series.
- Time-LLM [9]: Time-LLM introduces a reprogramming idea that aligns time series data with textual prototypes. Along with prefix prompts that provide descriptions and statistics of specific datasets, the reprogramming framework achieves cross-modal adaptation of LLMs for time series forecasting without any fine-tuning. For a fair comparison, this paper adopts GPT-2 as the backbone LLM for Time-LLM rather than its default setup (Llama-7B).
- GPT4TS [22]: GPT4TS leverages pre-trained LLMs for general time series analysis through a simple yet effective architecture called Frozen Pre-trained Transformer (FPT). FPT freezes the self-attention and feedforward layers while fine-tuning the layer normalization and positional embeddings, achieving promising performance across various time series tasks.

- TimeMixer [41]: TimeMixer proposes an MLP-based architecture designed to capture the multiscale temporal variations. Specifically, it decomposes and mixes the multiscale time series in both fine-to-coarse and coarse-to-fine directions, enabling comprehensive aggregation of microscopic and macroscopic information for time series learning.
- TimeXer [38]: TimeXer leverages the patch-level and variate-level representation ability, as well as the attention mechanism in Transformer, to model interactive dependencies between endogenous and exogenous variables, effectively capturing the causal relationships inherent in multivariate time series for forecasting.
- iTransformer [39]: iTransformer repurposes the canonical Transformer to focus on multivariate dependency modeling by inverting the embedding dimensions in the attention and feed-forward layers, achieving strong performance on real-world datasets.
- RLinear [17]: RLinear shows that a single linear layer, when combined with reversible normalization and channel independence techniques, can achieve efficient yet competitive performance compared to specialized and complex networks.
- PatchTST [40]: PatchTST introduces the concepts of patching and channel independence by segmenting time series into patches while preserving independence across variates. These designs enable Transformers to effectively capture both local and global dependencies, leading to improved performance.
- TimesNet [13]: TimesNet introduces a general time-series analysis approach based on frequency analysis and convolutional operations. It captures both intra-period and inter-period variations by transforming a 1D time series into a 2D representation.

Besides, a broader set of models is further employed for classification comparison, including Transformer-based models (Non-stationary Transformer [48], FlowFormer [49], Informer [50], Transformer [51]), MLP-based model (LightTS [52]), CNN-based model (TCN [53]), RNN-based models (LSSL [54], LSTNet [2]), and classical models (Rocket [55], XGBoost [56]). The details of the baselines are as follows.

- Non-stationary Transformer [48]: Non-stationary Transformer addresses the non-stationarity problem by employing stationary and de-stationary attention modules to restore and recover non-stationary information in time series, thereby improving the model's ability to distinguish temporal variations for forecasting.
- FlowFormer [49]: FlowFormer adopts a Transformer-based architecture inspired by optical flow estimation, utilizing a 4D cost volume to model fine-grained correspondences, which can be adapted for time series classification tasks.
- Informer [50]: Informer explores the sparsity of the attention mechanism to capture long-term temporal dependencies while reducing time and space complexity by identifying dominant features during attention operations.
- Transformer [51]: Transformer proposes an encoder-decoder architecture based on attention mechanisms to capture global dependencies in sequences, outperforming conventional RNNs/CNNs in speed and accuracy due to parallel processing and global context modeling.
- LightTS [52]: LightTS presents an efficient MLP-based framework that employs two distinct downsampling strategies to extract both short-term and long-term patterns in time series.
- TCN [53]: TCN introduces a deep neural network based on dilated causal convolutions, enabling efficient modeling of long-range dependencies in multivariate time series. In addition, it is trained in an unsupervised manner using a time-based triplet loss, which encourages similar subseries to have similar embeddings.
- LSSL [54]: LSSL introduces a structured state space model that reparameterizes state space models (SSMs) using a structured normal-plus-low-rank (NPLR) decomposition, enabling recurrent networks to effectively capture long-range dependencies in time series.
- LSTNet [2]: LSTNet is an autoregressive framework that combines a convolutional layer with a recurrent layer to capture short-term local dependencies and long-term periodic patterns with varying scales, enhancing the robustness of time series analysis.
- Rocket [55]: ROCKET is a classical time series classification method that transforms input sequences using thousands of randomly generated convolutional kernels, achieving state-of-the-art accuracy with significantly lower computational cost.

- XGBoost [56]: XGBoost builds upon traditional gradient tree boosting by improving sparsity handling and large-scale scalability, resulting in an efficient and flexible system applicable to a wide range of machine learning tasks, including time series analysis.

B.3 Implementation Details

All deep neural networks are implemented in PyTorch and trained on a Linux server (CPU: Intel(R) Xeon(R) Platinum 8452Y @ 2.00GHz, GPU: NVIDIA H800 GPU 80GB). To ensure fair comparisons, we adhere to the experimental configurations outlined in [13] to maintain a uniform evaluation procedure across all baselines. For baselines, we strictly follow their provided experimental settings or cite their performance if applicable [27, 41, 38].

Most of the training settings of our proposed framework are based on [22]. Specifically, we implement the proposed S^{2}TS-LLM using the first 4 layers of GPT-2 as the backbone LLM. Regarding the forecasting task, we train our S^{2}TS-LLM using the Adam optimizer with a learning rate of 0.0001, a decay rate $\beta = (0.9, 0.999)$, and a batch size of 256. A cosine annealing schedule with $T_{max} = 20$ and $\eta_{min} = 10^{-8}$ is used to adjust the model optimization. Early stopping is configured throughout the training process with a patience of 10. MSE loss is adopted for long-term forecasting, while SMAPE loss is used for short-term predictions. The top-k frequency in the spectral symbolization module is set to 5, and the segment score threshold γ in the contextual segmentation module is set to 0.1. The input time series is split into $G = 2$ slices for task prompt augmentation. Regarding the classification task, we train our S^{2}TS-LLM using the RAdam optimizer with a learning rate selected from $\{0.0005, 0.005\}$, and a cross-entropy loss is used for model optimization.

Regarding the metrics, we adopt the Mean Square Error (MSE) and Mean Absolute Error (MAE) for long-term forecasting. For the short-term forecasting, following [9], we adopt the Symmetric Mean Absolute Percentage Error (SMAPE), Mean Absolute Scaled Error (MASE), and Overall Weighted Average (OWA) as the metrics, where OWA is a special metric used in M4 competition. These metrics are defined as follows:

$$\text{MSE} = \frac{1}{H}\sum_{h=1}^{T}(\boldsymbol{Y}_l - \hat{\boldsymbol{Y}}_l)^2, \qquad \text{MAE} = \frac{1}{L_p}\sum_{l=1}^{L_p}|\boldsymbol{Y}_l - \hat{\boldsymbol{Y}}_l|,$$

$$\text{SMAPE} = \frac{200}{L_p}\sum_{l=1}^{L_p}\frac{|\boldsymbol{Y}_l - \hat{\boldsymbol{Y}}_l|}{|\boldsymbol{Y}_l| + |\hat{\boldsymbol{Y}}_l|}, \qquad \text{MAPE} = \frac{1}{L_p}\sum_{l=1}^{L_p}\frac{|\boldsymbol{Y}_l - \hat{\boldsymbol{Y}}_l|}{|\boldsymbol{Y}_l|},$$

$$\text{MASE} = \frac{1}{L_p}\sum_{l=1}^{L_p}\frac{|\boldsymbol{Y}_l - \hat{\boldsymbol{Y}}_l|}{\frac{1}{L_p - s}\sum_{j=s+1}^{L_p}|\boldsymbol{Y}_j - \boldsymbol{Y}_{j-s}|}, \qquad \text{OWA} = \frac{1}{2}\left[\frac{\text{SMAPE}}{\text{SMAPE}_{\text{Naïve2}}} + \frac{\text{MASE}}{\text{MASE}_{\text{Naïve2}}}\right].$$

C More Experiments

C.1 Analysis of Frequency Learning

Since the proposed method extracts spectral information to bootstrap LLMs' time-series comprehension, we further evaluate its frequency-domain learning capacity by examining magnitude sensitivity and trend preservation capability. Regarding magnitude sensitivity, we compute cosine similarity and Pearson correlation between the frequency components of predictions and ground truth. For trend preservation, we measure the dominant frequency overlap to assess how well each model captures underlying trends. Table 7 presents a comparative analysis of our S^{2}TS-LLM against two representative frequency-based models (FEDformer [18] and FiLM [16]), where our S^{2}TS-LLM consistently outperforms both baselines, demonstrating its effectiveness in preserving frequency-domain contributions for time-series modeling.

Table 7: Comparison of different methods in terms of magnitude sensitivity and trend preservation capability.

Dataset	Frequency Analysis		S^2TS-LLM (Ours)	FEDformer	FiLM
ETTh1	Magnitude Test	Cosine Similarity ↑	0.926	0.919	0.912
		Pearson Correlation ↑	0.878	0.865	0.857
	Trend Test	Dominant Frequency Overlap ↑	0.523	0.503	0.507
ETTh2	Magnitude Test	Cosine Similarity ↑	0.987	0.985	0.982
		Pearson Correlation ↑	0.985	0.982	0.979
	Trend Test	Dominant Frequency Overlap ↑	0.851	0.844	0.846

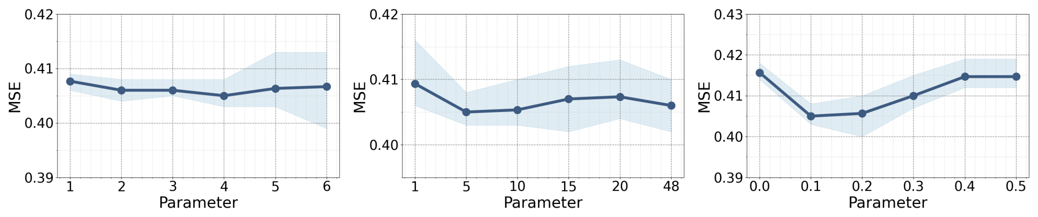

(a) Number of GPT-2 layers (b) Number of top-k frequencies (c) Segment score threshold

Figure 9: Sensitivity analysis of hyperparameters (a) number of GPT-2 layers, (b) number of top-k frequencies, and (c) segment score threshold on the ETTh1 dataset.

C.2 Hyperparameter Sensitivity

We perform a hyperparameter sensitivity analysis on the three key hyperparameters of the proposed S^2TS-LLM: the number of GPT-2 layers, the number of top-k frequencies, and the segment score threshold γ. This analysis is conducted on the ETTh1 dataset by averaging results across four prediction horizons $\{96, 192, 336, 720\}$ under different hyperparameter settings. Figure 9 presents the results averaged over three independent runs for each hyperparameter, where the dark blue lines represent the average results from three runs and the light blue boundaries indicate the error bars.

- **Number of GPT-2 layers.** GPT-2 typically consists of 12 transformer layers. We assess the impact of GPT-2 network depth by varying the number of layers from 1 to 6. As shown in Figure 9(a), our S^2TS-LLM exhibits low sensitivity to the number of layers. This can be attributed to the use of minimalist symbolic abstractions, which effectively align time series with natural language and reduce the reliance on deep LLM layers for multimodal understanding. While increasing the number of layers can reduce prediction error, deeper models may introduce the overfitting problem, leading to unstable results—as evidenced by the 6-layer variant, which shows the lowest MSE but the highest variance. To trade off performance and computational efficiency, we adopt the first 4 layers of GPT-2 as the backbone LLM in our framework.
- **Number of top-k frequencies.** Due to the symmetry of the Fast Fourier Transform, the number of top-k frequencies is selected from the candidate set $\{1, 5, 10, 15, 20, 24\}$, ensuring it does not exceed half the feature dimension of the patched input $\hat{\boldsymbol{X}}$ (48 dimensions, as used in [22]). As depicted in Figure 9 (b), neither too few nor too many top-k frequencies lead to satisfactory results: a smaller k fails to capture sufficient frequency patterns, while a larger k introduces noisy spectral components. Based on this analysis, we set $k = 5$ to achieve the best performance.
- **Segment score threshold.** We select the segment score threshold γ from the range $[0.0, 0.5]$, and the sensitivity results are illustrated in Figure 9 (c). When $\gamma = 0$, each input patch is treated as an individual segment, disabling the contextual segmentation mechanism and resulting in the worst performance. As γ increases to 0.5, the segmentation tends to form overly long segments or even a single segment for the entire input, which diminishes the structural granularity of the time series and leads to performance degradation. Based on these observations, we set $\gamma = 0.1$ to achieve optimal performance.

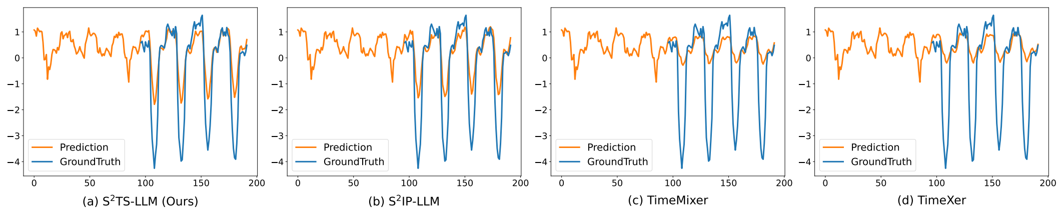

Figure 10: Long-term forecasting cases from ETTh1 by different models under the input-96-predict-96 settings. Blue lines are the ground truths and orange lines are the model predictions.

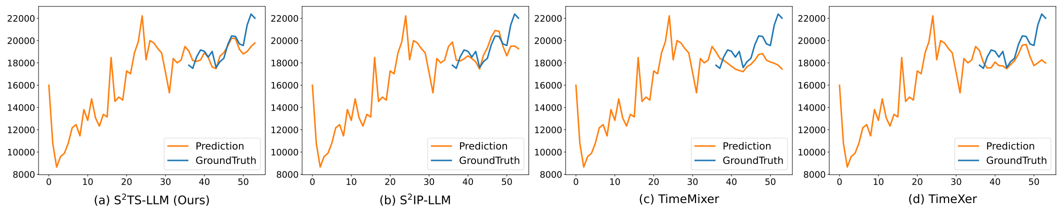

Figure 11: Short-term forecasting cases from the M4 dataset by different models under the input-36-predict-18 settings. Blue lines are the ground truths and orange lines are the model predictions.

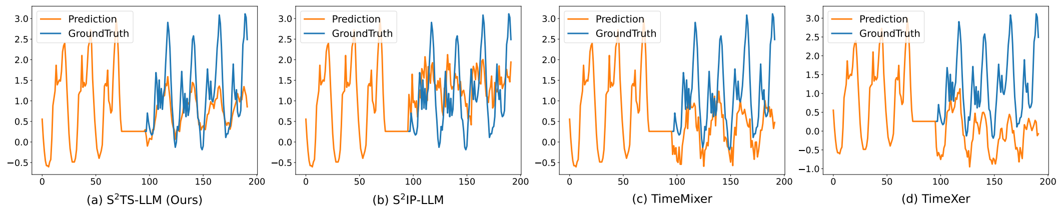

Figure 12: Few-shot forecasting cases from ETTh1 by different models under the input-96-predict-96 settings. Blue lines are the ground truths and orange lines are the model predictions.

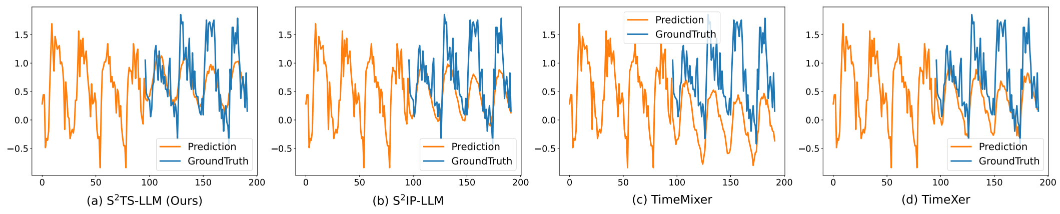

Figure 13: Zero-shot forecasting cases from ETTh2$\rightarrow$ETTh1 by different models under the input-96-predict-96 settings. Blue lines are the ground truths and orange lines are the model predictions.

C.3 Forecasting Visualization

To evaluate the forecasting capabilities of the proposed S^{2}TS-LLM, Figures 10 to 13 present visualization examples across long-term forecasting, short-term forecasting, few-shot learning, and zero-shot learning tasks, which are compared against baseline models, including S^{2}IP-LLM [7], TimeMixer [41], and TimeXer [38]. We observe that the datasets exhibit complex variations that pose significant challenges for prediction. For instance, the ETTh1 example in Figure 10 begins with regular periodic fluctuations, followed by a sequence of abrupt drops and spikes. Despite such complexity, the visualizations demonstrate that S^{2}TS-LLM achieves good predictive performance across various tasks. This is especially evident in few-shot and zero-shot scenarios, where S^{2}TS-LLM successfully captures future trends, whereas the baseline models often struggle.

Table 8: Training parameters and Training/Inference Cost Comparison

Type	Model	Training Params	Training Params Percentage (%)	Training Time per Step (s)	Inference Time per Batch (s)
Conventional Specialized Model	TimesNet-32	4.77M	100	0.207	0.156
	TimesNet-768	107.63M	100	1.020	0.856
LLM-based Model	GPT4TS(4)-768	1.57M	2	0.029	0.031
	Time-LLM(4)-768	54.25M	46	0.551	0.941
	S^{2}IP-LLM(4)-768	49.15M	44	0.562	1.202
	S^{2}TS-LLM(4)-768 (Ours)	2.71M	4	0.158	0.189

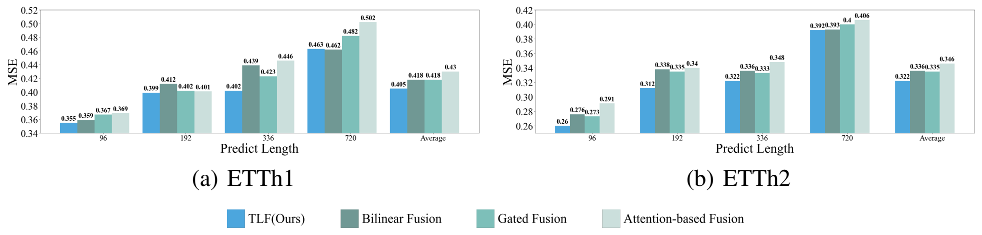

Figure 14: Comparison of different fusion strategy on the ETTh1 and ETTh2 datasets, where lower MSE values indicate better performance.

C.4 Computational Cost

The computational cost is a critical factor in assessing the practicality of LLM-based models. To evaluate this, we compare our S^{2}TS-LLM with a specialized model (TimesNet) and three LLM-based models (GPT4TS, Time-LLM, and S^{2}IP-LLM) in terms of training and inference costs. Specifically, TimesNet is tested in two setups with embedding dimensions of 32 and 768, the latter matching the embedding size of GPT-2. Regarding the LLM-based baselines, the default settings of LLM-based S^{2}IP-LLM, Time-LLM, and GPT4TS utilize the first 6, 12, and 6 hidden layers of GPT-2, respectively. To ensure a fair comparison, we uniformly configure all LLM-based baselines with 4 layers, consistent with the architecture of our proposed model. The computational cost analysis is conducted on the ETTh1 dataset with a batch size of 128, using an 80G H800 GPU.

As shown in Table 8, our S^{2}TS-LLM achieves competitive efficiency and parameter count compared to baseline methods. Particularly, our S^{2}TS-LLM outperforms TimesNet in training efficiency while delivering superior forecasting accuracy, underscoring the practicality of our approach. Compared to LLM-based methods, S^{2}TS-LLM incurs a slightly higher computational cost than GPT4TS, primarily due to the additional overhead introduced by our cross-modal alignment and prompt augmentation. Importantly, while sharing the same objective of cross-modal alignment with S^{2}IP-LLM and Time-LLM, our method achieves superior computational and memory efficiency. This highlights that the sparsity inherent in frequency-domain signals can significantly reduce the complexity of aligning time series with natural language, validating the efficacy of our spectral symbolization paradigm.

C.5 Effectiveness of Time-Linguistic Fusion

Inspire by the RNNs, our Time-Linguistic Fusion (TLF) adopts a gated residual update mechanism ($\boldsymbol{O}^{(n)} = \boldsymbol{O}_X^{(n)} + \boldsymbol{A}^{(n)} \odot \sigma(\boldsymbol{O}_T^{(n)}) \odot \boldsymbol{O}_X^{(n)}$) to fuse textual and time-series outputs. To assess the effectiveness of this design, we compare it against several alternative fusion strategies, including bilinear fusion ($z = x^T W y$), gated fusion ($z = \alpha x + (1 - \alpha) y$), and attention-based fusion (Softmax $\left(\frac{(yW_Q)(xW_K)^T}{\sqrt{d}}(xW_V)\right)$), where $x = O_X^{(n)}$ and $y = O_T^{(n)}$. MSE results in Figure 14 demonstrate that our proposed TLF consistently outperforms these alternatives. This superior performance arises because the sigmoid function $\sigma(\cdot)$ softly modulates frequency information by smoothly mapping spectral features into a bounded embedding space $(0, 1)$, rather than discarding them. Furthermore, the residual fusion strategy is particularly well-suited for integrating auxiliary frequency cues with raw numerical features: frequency-domain signals guide LLMs semantically

Table 9: Performance comparison of different methods across varying lookback lengths.

Dataset	Lookback Length	512		336		192		96		48	
	Metric	MSE↓	MAE↓	MSE↓	MAE↓	MSE↓	MAE↓	MSE↓	MAE↓	MSE↓	MAE↓
ETTh1	S^2TS-LLM (Ours)	0.355	0.387	0.365	0.389	0.372	0.391	0.378	0.391	0.398	0.411
	S^2IP-LLM	0.368	0.403	0.367	0.398	0.368	0.393	0.379	0.394	0.390	0.401
	GPT4TS	0.376	0.397	0.378	0.399	0.380	0.401	0.383	0.401	0.385	0.403
ETTh2	S^2TS-LLM (Ours)	0.260	0.329	0.281	0.335	0.288	0.338	0.291	0.336	0.310	0.350
	S^2IP-LLM	0.284	0.345	0.282	0.343	0.288	0.343	0.293	0.343	0.301	0.344
	GPT4TS	0.285	0.342	0.286	0.345	0.294	0.349	0.295	0.349	0.299	0.350

rather than numerically, and residual pathways enable smoother integration without disrupting the structure of the original signal.

C.6 Analysis of Performance Gain

To investigate when our S^2STS-LLM works well and when it fails, we follow prior work [9, 19] to evaluate model performance under different lookback lengths $\{512, 336, 192, 96, 48\}$. The detailed MSE results on the ETTh1 and ETTh2 datasets are shown in Table 9. We observe that S^2STS-LLM outperforms the other two LLM-based methods, S^2IP-LLM and GPT4TS, when the lookback length is between 512 and 96. However, as the lookback length decreases to 48, S^2STS-LLM experiences a significant performance drop and underperforms compared to the S^2IP-LLM and GPT4TS. This is consistent with Table 2's observation that S^2STS-LLM achieves suboptimal results on short-term forecasting tasks. The main reason is that S^2STS-LLM uses FFT to extract dominant frequency components, which leads to further information compression when the lookback window is short. As a result, the generated compact textual descriptions may not provide LLMs with sufficient information to bridge the semantic gap between linguistics and time series. Therefore, our method is better suited for long-sequence scenarios. For example, our model shows significant gains in both long-term forecasting and zero-shot learning tasks (refer to Tables 1 and 4), where it can capture enough dominant frequency components to distinguish different temporal patterns.

D Discussion

Impact Statement. This work presents a step forward in time series forecasting by exploring how time series data can be aligned with the representational space and contextual structures of the LLMs. Our proposed frequency-based alignment approach offers a compact and efficient alternative for cross-modal adaptation, highlighting the potential of leveraging the frequency domain rather than the time domain for time-series-driven LLMs. Beyond representation, our study also underscores the value of contextual alignment in adapting LLMs to time series tasks. We believe that as the LLMs develop a deeper understanding of time series, conventional time series analysis will gradually advance toward a more universal form of artificial intelligence. In particular, the extensive internal knowledge and reasoning capabilities of LLMs hold great promise for addressing complex time series tasks and improving decision-making across critical domains such as finance, healthcare, and environmental monitoring.

Limitation and Future Work. S^2TS-LLM demonstrates favorable performance and reasonable efficiency across various time series analysis tasks, including forecasting and classification. However, we observe that the use of time–frequency transformation may intensify to information compression when the input sequence is relatively short, resulting in performance degradation (refer to Table 2 and Table 9). To address this limitation, future work will explore alternative frequency representations to augment frequency information, such as multi-scale fusion of frequency features or contrastive learning across different frequency views. Moreover, this study focuses solely on cross-modal alignment between time series and linguistics, neglecting the visual modality of time series. Incorporating time series, computer vision, and natural language into a unified multi-modal framework is a promising direction. Lastly, given its application-oriented design, we plan to extend S^2TS-LLM to broader tasks such as anomaly detection, imputation, and spatio-temporal analysis, while further improving its computational efficiency to enhance practical value.

Table 10: Full long-term forecasting results. The prediction horizons are set to $\{96, 192, 336, 720\}$. A lower value indicates better performance. Red denotes the best performance, while Blue indicates the second-best.

Methods		S^2TS-LLM		S^2 IP-LLM		Time-LLM		GPT4TS		TimeMixer		TimeXer		iTransformer		RLinear		PatchTST		TimesNet	
Metric		MSE	MAE	MSE	MAE	MSE	MAE	MSE	MAE	MSE	MAE	MSE	MAE	MSE	MAE	MSE	MAE	MSE	MAE	MSE	MAE
Weather	96	0.148	0.200	0.149	0.200	0.163	0.210	0.162	0.212	0.163	0.209	0.157	0.205	0.174	0.214	0.192	0.232	0.177	0.218	0.172	0.220
	192	0.191	0.241	0.195	0.244	0.205	0.245	0.204	0.248	0.208	0.250	0.204	0.247	0.221	0.254	0.240	0.271	0.225	0.259	0.219	0.261
	336	0.244	0.283	0.246	0.280	0.257	0.287	0.254	0.286	0.251	0.287	0.261	0.290	0.278	0.296	0.292	0.307	0.278	0.297	0.280	0.306
	720	0.319	0.338	0.320	0.336	0.323	0.332	0.326	0.337	0.339	0.341	0.340	0.341	0.358	0.349	0.364	0.353	0.354	0.348	0.365	0.359
	Avg	0.225	0.265	0.228	0.265	0.237	0.269	0.237	0.270	0.240	0.271	0.241	0.271	0.258	0.278	0.272	0.291	0.259	0.281	0.259	0.287
ECL	96	0.133	0.228	0.138	0.234	0.140	0.236	0.139	0.238	0.153	0.247	0.140	0.242	0.148	0.240	0.201	0.281	0.195	0.285	0.168	0.272
	192	0.151	0.245	0.153	0.252	0.150	0.249	0.153	0.251	0.166	0.256	0.157	0.256	0.162	0.253	0.201	0.283	0.199	0.289	0.184	0.289
	336	0.168	0.261	0.169	0.270	0.168	0.267	0.169	0.266	0.185	0.277	0.176	0.275	0.178	0.269	0.215	0.298	0.215	0.305	0.198	0.300
	720	0.205	0.291	0.204	0.293	0.209	0.302	0.206	0.297	0.225	0.310	0.211	0.306	0.225	0.317	0.257	0.331	0.256	0.337	0.220	0.320
	Avg	0.164	0.256	0.166	0.262	0.167	0.264	0.167	0.263	0.182	0.272	0.171	0.270	0.178	0.270	0.219	0.298	0.216	0.304	0.192	0.295
Traffic	96	0.364	0.263	0.379	0.274	0.384	0.278	0.388	0.282	0.462	0.285	0.428	0.271	0.395	0.268	0.649	0.389	0.462	0.295	0.593	0.321
	192	0.389	0.275	0.397	0.282	0.398	0.286	0.407	0.290	0.473	0.296	0.448	0.282	0.417	0.276	0.601	0.366	0.466	0.296	0.617	0.336
	336	0.395	0.275	0.407	0.289	0.408	0.289	0.412	0.294	0.498	0.296	0.473	0.289	0.433	0.283	0.609	0.369	0.482	0.304	0.629	0.336
	720	0.436	0.297	0.440	0.301	0.436	0.303	0.450	0.312	0.506	0.313	0.516	0.307	0.467	0.302	0.647	0.387	0.514	0.322	0.640	0.350
	Avg	0.396	0.278	0.405	0.286	0.407	0.289	0.414	0.294	0.484	0.297	0.466	0.287	0.428	0.282	0.626	0.378	0.481	0.304	0.620	0.336
ETTh1	96	0.355	0.387	0.367	0.398	0.383	0.404	0.376	0.397	0.375	0.400	0.382	0.403	0.386	0.405	0.386	0.395	0.414	0.419	0.384	0.402
	192	0.399	0.419	0.402	0.422	0.427	0.431	0.416	0.418	0.429	0.421	0.429	0.435	0.441	0.436	0.437	0.424	0.460	0.445	0.436	0.429
	336	0.402	0.432	0.432	0.451	0.430	0.436	0.442	0.433	0.484	0.458	0.468	0.448	0.487	0.458	0.479	0.446	0.501	0.466	0.491	0.469
	720	0.463	0.478	0.472	0.474	0.465	0.469	0.477	0.456	0.498	0.482	0.469	0.461	0.503	0.491	0.481	0.470	0.500	0.488	0.521	0.500
	Avg	0.404	0.429	0.418	0.436	0.426	0.435	0.427	0.426	0.447	0.440	0.437	0.437	0.454	0.447	0.446	0.434	0.469	0.454	0.458	0.450
ETTh2	96	0.260	0.329	0.284	0.345	0.293	0.348	0.285	0.342	0.289	0.341	0.286	0.338	0.297	0.349	0.288	0.338	0.302	0.348	0.340	0.374
	192	0.312	0.363	0.349	0.387	0.356	0.391	0.354	0.389	0.372	0.392	0.363	0.389	0.380	0.400	0.374	0.390	0.388	0.400	0.402	0.414
	336	0.322	0.380	0.368	0.417	0.372	0.408	0.373	0.407	0.386	0.414	0.414	0.423	0.428	0.432	0.415	0.426	0.426	0.433	0.452	0.452
	720	0.392	0.430	0.419	0.445	0.421	0.446	0.406	0.441	0.412	0.434	0.408	0.432	0.427	0.445	0.420	0.440	0.431	0.446	0.462	0.468
	Avg	0.321	0.376	0.355	0.399	0.361	0.398	0.354	0.394	0.364	0.395	0.367	0.396	0.383	0.407	0.374	0.398	0.387	0.407	0.414	0.427
ETTm1	96	0.282	0.343	0.291	0.348	0.294	0.345	0.292	0.346	0.320	0.357	0.318	0.356	0.334	0.368	0.355	0.376	0.329	0.367	0.338	0.375
	192	0.322	0.368	0.323	0.368	0.330	0.368	0.332	0.372	0.361	0.381	0.362	0.383	0.387	0.391	0.391	0.392	0.367	0.385	0.374	0.387
	336	0.356	0.388	0.361	0.392	0.365	0.392	0.366	0.394	0.390	0.404	0.395	0.407	0.426	0.420	0.424	0.415	0.399	0.410	0.410	0.411
	720	0.416	0.419	0.410	0.420	0.427	0.431	0.417	0.421	0.454	0.441	0.452	0.441	0.491	0.459	0.487	0.450	0.454	0.439	0.478	0.450
	Avg	0.344	0.380	0.346	0.382	0.354	0.384	0.352	0.383	0.381	0.395	0.382	0.397	0.407	0.410	0.414	0.407	0.387	0.400	0.400	0.406
ETTm2	96	0.169	0.259	0.167	0.257	0.175	0.265	0.173	0.262	0.175	0.258	0.171	0.256	0.180	0.264	0.182	0.265	0.175	0.259	0.187	0.267
	192	0.225	0.297	0.227	0.303	0.243	0.316	0.229	0.301	0.237	0.299	0.237	0.299	0.250	0.309	0.246	0.304	0.241	0.302	0.249	0.309
	336	0.277	0.331	0.285	0.346	0.294	0.343	0.286	0.341	0.298	0.340	0.296	0.338	0.311	0.348	0.307	0.342	0.305	0.343	0.321	0.351
	720	0.362	0.386	0.368	0.398	0.389	0.410	0.378	0.401	0.391	0.396	0.392	0.394	0.412	0.407	0.407	0.398	0.402	0.400	0.408	0.403
	Avg	0.258	0.318	0.262	0.326	0.275	0.334	0.266	0.326	0.275	0.323	0.274	0.322	0.288	0.332	0.286	0.327	0.281	0.326	0.291	0.333
Average		0.302	0.329	0.311	0.337	0.318	0.339	0.317	0.337	0.339	0.342	0.334	0.340	0.342	0.347	0.377	0.362	0.354	0.354	0.376	0.362

E Full Results

Here, we provide the full results of each experiment listed in the main text, including long-term/short-term forecasting, few-shot/zero-shot learning, time series classification, and ablation study.

E.1 Long-term Forecasting

Table 10 presents the detailed long-term forecasting results across four prediction horizons $\{96, 192, 336, 720\}$ on seven widely used datasets. S^2TS-LLM consistently outperforms the high-performing baselines, achieving an average reduction of 2.9% in MSE and 2.5% in MAE compared to the second-best method, S^2IP-LLM [7]. These results validate the effectiveness of our representational and contextual alignment between time series and natural language.

E.2 Short-term Forecasting

Table 11 illustrates the detailed short-term forecasting results on six M4 datasets. In this setting, prediction horizons range from 6 to 48, with input lengths set to twice the horizon. While our S^2TS-LLM achieves the best performance among LLM-based methods, including S^2IP-LLM [7], Time-LLM [9], and GPT4TS [22], it performs slightly below the lightweight model TimeMixer [41]. This may be due to the relatively short input sequences (ranging from 12 to 96), which limit the ability of LLMs to effectively model long-range dependencies.

E.3 Few-shot Learning

Tables 12 and 13 provide the detailed few-shot forecasting results trained on the first 5% and 10% of the data, respectively, across various prediction lengths. The proposed S^2TS-LLM consistently

Table 11: Full short-term forecasting results. The prediction horizons are in $[6, 48]$, and the last three rows are weighted averaged from all datasets under different sampling intervals. A lower value indicates better performance. Red denotes the best performance, while Blue indicates the second-best.

	Methods	S^{2}TS-LLM	S^{2}IP-LLM	Time-LLM	GPT4TS	TimeMixer	TimeXer	iTransformer	RLinear	PatchTST	TimesNet
Year.	SMAPE	13.306	13.413	13.750	15.110	13.206	13.370	13.652	13.617	13.477	15.378
	MASE	3.007	3.024	3.055	3.565	2.916	3.002	3.095	2.991	3.019	3.554
	OWA	0.785	0.792	0.805	0.911	0.776	0.787	0.807	0.793	0.792	0.918
Quart.	SMAPE	10.242	10.352	10.671	10.597	9.996	10.323	10.353	10.752	10.380	10.465
	MASE	1.209	1.228	1.276	1.253	1.166	1.221	1.209	1.313	1.233	1.227
	OWA	0.906	0.922	0.950	0.938	0.825	0.914	0.911	0.967	0.921	0.923
Month.	SMAPE	12.967	12.995	13.416	13.258	12.605	13.076	13.079	13.338	12.959	13.513
	MASE	0.975	0.970	1.045	1.003	0.919	0.977	0.974	1.027	0.970	1.039
	OWA	0.908	0.910	0.957	0.931	0.869	0.912	0.911	0.945	0.905	0.957
Others.	SMAPE	4.837	4.805	4.973	6.124	4.564	5.054	4.780	4.979	4.952	6.913
	MASE	3.310	3.247	3.412	4.116	3.115	3.373	3.231	3.332	3.347	4.507
	OWA	1.031	1.017	1.053	1.259	0.982	1.064	1.012	1.049	1.049	1.438
Avg.	SMAPE	11.979	12.021	12.494	12.690	11.723	12.082	12.142	12.363	12.059	12.880
	MASE	1.610	1.612	1.731	1.808	1.559	1.621	1.631	1.662	1.623	1.836
	OWA	0.862	0.857	0.913	0.940	0.840	0.874	0.869	0.890	0.869	0.955

Table 12: Full few-shot learning results on 5% training data. We use the same protocol as in Table 10.

Methods		S^{2}TS-LLM		S^{2}IP-LLM		Time-LLM		GPT4TS		TimeMixer		TimeXer		iTransformer		RLinear		PatchTST		TimesNet	
Metric		MSE	MAE	MSE	MAE	MSE	MAE	MSE	MAE	MSE	MAE	MSE	MAE	MSE	MAE	MSE	MAE	MSE	MAE	MSE	MAE
ETTh1	96	0.482	0.447	0.500	0.493	0.518	0.498	0.543	0.506	0.558	0.502	0.496	0.469	0.808	0.610	0.501	0.474	0.557	0.519	0.892	0.625
	192	0.529	0.485	0.690	0.539	0.702	0.547	0.748	0.580	0.764	0.607	0.724	0.609	0.928	0.658	0.677	0.566	0.711	0.570	0.940	0.665
	336	0.730	0.577	0.761	0.620	0.725	0.603	0.754	0.595	0.855	0.644	0.934	0.662	1.475	0.861	0.876	0.638	0.816	0.619	0.945	0.653
	720	-	-	-	-	-	-	-	-	-	-	-	-	-	-						
	Avg	0.580	0.503	0.650	0.550	0.648	0.549	0.681	0.560	0.726	0.584	0.718	0.580	1.070	0.710	0.685	0.559	0.695	0.569	0.925	0.647
ETTh2	96	0.303	0.347	0.363	0.409	0.384	0.420	0.376	0.421	0.369	0.393	0.334	0.369	0.397	0.427	0.344	0.377	0.401	0.421	0.409	0.420
	192	0.360	0.395	0.375	0.411	0.394	0.424	0.418	0.441	0.451	0.439	0.461	0.444	0.438	0.445	0.505	0.459	0.452	0.455	0.483	0.464
	336	0.419	0.441	0.403	0.421	0.416	0.433	0.408	0.439	0.492	0.479	0.755	0.603	0.631	0.553	0.538	0.493	0.464	0.469	0.499	0.479
	720	-	-	-	-	-	-	-	-	-	-	-	-	-	-						
	Avg	0.360	0.394	0.380	0.413	0.398	0.426	0.400	0.433	0.437	0.437	0.517	0.472	0.488	0.475	0.462	0.443	0.439	0.448	0.463	0.454
ETTm1	96	0.440	0.423	0.357	0.390	0.422	0.424	0.386	0.405	0.563	0.484	0.509	0.462	0.589	0.510	0.426	0.425	0.399	0.414	0.606	0.518
	192	0.434	0.422	0.432	0.434	0.448	0.440	0.440	0.438	0.579	0.490	0.538	0.472	0.703	0.565	0.455	0.440	0.441	0.436	0.681	0.539
	336	0.455	0.440	0.440	0.442	0.452	0.447	0.485	0.459	0.599	0.510	0.597	0.512	0.898	0.641	0.514	0.479	0.499	0.467	0.786	0.597
	720	0.568	0.502	0.593	0.521	0.585	0.491	0.577	0.499	0.886	0.648	0.831	0.637	0.948	0.671	0.707	0.565	0.767	0.587	0.796	0.593
	Avg	0.474	0.447	0.455	0.446	0.477	0.451	0.472	0.450	0.657	0.533	0.619	0.521	0.784	0.596	0.526	0.477	0.526	0.476	0.717	0.561
ETTm2	96	0.197	0.280	0.197	0.278	0.205	0.277	0.199	0.280	0.199	0.282	0.203	0.287	0.265	0.339	0.193	0.273	0.206	0.288	0.220	0.299
	192	0.257	0.319	0.254	0.322	0.267	0.336	0.256	0.316	0.262	0.320	0.265	0.325	0.310	0.362	0.265	0.319	0.264	0.324	0.311	0.361
	336	0.302	0.344	0.315	0.350	0.309	0.347	0.318	0.353	0.331	0.361	0.331	0.362	0.373	0.399	0.323	0.352	0.334	0.367	0.338	0.366
	720	0.414	0.410	0.421	0.421	0.448	0.432	0.460	0.436	0.502	0.463	0.480	0.445	0.478	0.454	0.461	0.435	0.454	0.432	0.509	0.465
	Avg	0.293	0.338	0.296	0.342	0.307	0.348	0.308	0.346	0.324	0.357	0.320	0.355	0.356	0.388	0.311	0.345	0.314	0.352	0.344	0.372
Average		0.427	0.421	0.445	0.438	0.458	0.444	0.465	0.447	0.605	0.511	0.606	0.509	0.675	0.542	0.496	0.456	0.494	0.461	0.612	0.509

outperforms the baselines on most datasets, with the exception of ETTm1. Given the inherent sparsity and variability in few-shot learning scenarios, such performance differences on specific datasets are within a reasonable and acceptable range. Additionally, the results show that almost all LLM-based methods outperform conventional specialized models, highlighting the strong few-shot learning capabilities of large language models.

E.4 Zero-shot Learning

Table 14 reports the detailed results of the zero-shot forecasting task across various prediction lengths. S^{2}TS-LLM almost achieves the best performance across all settings, delivering a notable 8.3% improvement over the second-best method, RLinear. Interestingly, RLinear performs surprisingly well, possibly because its simple linear structure mitigates overfitting to the source dataset, enhancing generalization in the zero-shot setting. Different from RLinear, our S^{2}TS-LLM effectively activates the internal knowledge of LLMs to facilitate cross-domain adaptation from source to target datasets.

E.5 Time Series Classification

Table 15 presents the comparative results on 10 multivariate UEA classification datasets. For the time series classification task, we include a diverse set of baselines tailored for time series classification, including classical models (XGBoost [56], Rocket [55]), RNN-based models (LSSL [54], LSTNet [2]), Transformer-based models (Transformer [51], Informer [50], Non-stationary

Table 13: Full few-shot learning results on 10% training data. We use the same protocol as in Table 10.

Methods		S^2TS-LLM		S^2IP-LLM		Time-LLM		GPT4TS		TimeMixer		TimeXer		iTransformer		RLinear		PatchTST		TimesNet	
Metric		MSE	MAE	MSE	MAE	MSE	MAE	MSE	MAE	MSE	MAE	MSE	MAE	MSE	MAE	MSE	MAE	MSE	MAE	MSE	MAE
ETTh1	96	0.469	0.444	0.481	0.474	0.720	0.533	0.458	0.456	0.513	0.477	0.483	0.461	0.790	0.586	0.447	0.442	0.516	0.485	0.861	0.628
	192	0.493	0.472	0.518	0.491	0.747	0.545	0.570	0.516	0.571	0.507	0.549	0.481	0.837	0.609	0.544	0.492	0.598	0.524	0.797	0.593
	336	0.533	0.494	0.664	0.570	0.793	0.551	0.608	0.535	0.713	0.570	0.716	0.570	0.780	0.575	0.671	0.559	0.657	0.550	0.941	0.648
	720	0.678	0.560	0.711	0.584	0.880	0.584	0.725	0.591	1.004	0.717	0.991	0.697	1.234	0.811	0.839	0.636	0.762	0.610	0.877	0.641
	Avg	0.543	0.493	0.593	0.529	0.785	0.553	0.590	0.525	0.700	0.568	0.685	0.552	0.910	0.860	0.625	0.532	0.633	0.542	0.869	0.628
ETTh2	96	0.305	0.349	0.354	0.400	0.334	0.381	0.331	0.374	0.338	0.375	0.330	0.365	0.404	0.435	0.328	0.362	0.353	0.389	0.378	0.409
	192	0.353	0.391	0.401	0.423	0.430	0.438	0.402	0.411	0.405	0.406	0.412	0.410	0.470	0.474	0.420	0.418	0.403	0.414	0.490	0.467
	336	0.392	0.420	0.442	0.450	0.449	0.458	0.406	0.433	0.475	0.463	0.498	0.467	0.489	0.485	0.516	0.476	0.426	0.441	0.537	0.494
	720	0.437	0.446	0.480	0.486	0.485	0.490	0.449	0.464	0.605	0.539	0.654	0.564	0.593	0.538	0.587	0.517	0.477	0.480	0.510	0.491
	Avg	0.372	0.402	0.419	0.439	0.424	0.441	0.397	0.421	0.456	0.446	0.474	0.451	0.489	0.483	0.463	0.443	0.415	0.431	0.479	0.465
ETTm1	96	0.432	0.421	0.388	0.401	0.412	0.422	0.390	0.404	0.552	0.479	0.492	0.461	0.709	0.556	0.398	0.411	0.410	0.419	0.583	0.501
	192	0.436	0.421	0.422	0.421	0.447	0.438	0.429	0.423	0.571	0.492	0.525	0.465	0.717	0.548	0.430	0.426	0.437	0.434	0.630	0.528
	336	0.460	0.431	0.456	0.430	0.497	0.465	0.469	0.439	0.580	0.503	0.538	0.483	0.735	0.575	0.464	0.446	0.476	0.454	0.725	0.568
	720	0.530	0.472	0.554	0.490	0.594	0.521	0.569	0.498	0.687	0.534	0.671	0.515	0.752	0.584	0.528	0.472	0.681	0.556	0.769	0.549
	Avg	0.465	0.436	0.455	0.435	0.487	0.461	0.464	0.441	0.598	0.502	0.557	0.481	0.728	0.565	0.455	0.439	0.501	0.466	0.677	0.537
ETTm2	96	0.188	0.272	0.192	0.274	0.224	0.296	0.188	0.269	0.189	0.269	0.196	0.279	0.245	0.322	0.183	0.260	0.191	0.274	0.212	0.285
	192	0.248	0.308	0.246	0.313	0.260	0.317	0.251	0.309	0.255	0.308	0.252	0.309	0.274	0.338	0.250	0.303	0.252	0.317	0.270	0.323
	336	0.295	0.338	0.301	0.340	0.312	0.349	0.307	0.346	0.310	0.345	0.318	0.351	0.361	0.394	0.313	0.343	0.306	0.353	0.323	0.353
	720	0.383	0.390	0.400	0.403	0.424	0.416	0.426	0.417	0.448	0.421	0.457	0.431	0.467	0.442	0.433	0.413	0.433	0.427	0.474	0.449
	Avg	0.279	0.327	0.284	0.332	0.305	0.344	0.293	0.335	0.301	0.336	0.306	0.343	0.336	0.373	0.295	0.330	0.296	0.343	0.320	0.353
Average		0.415	0.415	0.438	0.434	0.500	0.450	0.436	0.431	0.562	0.478	0.513	0.460	0.616	0.570	0.460	0.436	0.461	0.446	0.586	0.496

Table 14: Full zero-shot learning results on ETT datasets. A lower value indicates better performance. Red denotes the best performance, while Blue indicates the second-best.

Methods		S^2TS-LLM		S^2IP-LLM		Time-LLM		GPT4TS		TimeMixer		TimeXer		iTransformer		RLinear		PatchTST		TimesNet	
Metric		MSE	MAE	MSE	MAE	MSE	MAE	MSE	MAE	MSE	MAE	MSE	MAE	MSE	MAE	MSE	MAE	MSE	MAE	MSE	MAE
ETTh1 ↓ ETTh2	96	0.279	0.339	0.315	0.377	0.324	0.368	0.335	0.374	0.297	0.346	0.308	0.351	0.353	0.394	0.296	0.342	0.304	0.350	0.358	0.387
	192	0.336	0.378	0.402	0.407	0.398	0.396	0.412	0.417	0.376	0.390	0.391	0.404	0.437	0.445	0.383	0.394	0.386	0.400	0.427	0.429
	336	0.362	0.402	0.453	0.432	0.410	0.423	0.441	0.444	0.411	0.420	0.439	0.436	0.482	0.476	0.420	0.428	0.414	0.428	0.449	0.451
	720	0.387	0.427	0.442	0.451	0.403	0.449	0.438	0.452	0.410	0.432	0.421	0.437	0.556	0.506	0.420	0.438	0.419	0.443	0.448	0.458
	Avg	0.341	0.387	0.403	0.417	0.384	0.409	0.406	0.422	0.374	0.397	0.390	0.407	0.457	0.455	0.380	0.401	0.380	0.405	0.421	0.431
ETTh1 ↓ ETTm2	96	0.209	0.300	0.242	0.319	0.236	0.320	0.236	0.315	0.228	0.311	0.233	0.313	0.247	0.319	0.218	0.300	0.215	0.304	0.239	0.313
	192	0.260	0.330	0.286	0.337	0.265	0.353	0.287	0.342	0.278	0.337	0.286	0.343	0.293	0.350	0.277	0.335	0.275	0.339	0.291	0.342
	336	0.312	0.360	0.351	0.367	0.337	0.376	0.341	0.374	0.341	0.375	0.364	0.386	0.364	0.419	0.335	0.368	0.334	0.373	0.342	0.371
	720	0.394	0.409	0.422	0.416	0.429	0.430	0.435	0.422	0.436	0.424	0.437	0.423	0.534	0.470	0.432	0.420	0.431	0.424	0.434	0.419
	Avg	0.294	0.350	0.325	0.360	0.317	0.370	0.325	0.363	0.321	0.362	0.330	0.366	0.360	0.390	0.316	0.356	0.314	0.360	0.327	0.361
ETTh2 ↓ ETTh1	96	0.509	0.478	0.668	0.567	0.618	0.515	0.732	0.577	0.476	0.459	0.507	0.477	0.854	0.606	0.455	0.444	0.485	0.465	0.848	0.601
	192	0.543	0.507	0.575	0.526	0.715	0.570	0.758	0.559	0.765	0.595	0.591	0.522	0.863	0.615	0.513	0.477	0.565	0.509	0.860	0.610
	336	0.558	0.517	0.655	0.577	0.636	0.523	0.759	0.578	0.678	0.558	0.705	0.579	0.867	0.626	0.606	0.524	0.581	0.515	0.867	0.626
	720	0.590	0.551	0.778	0.568	0.683	0.553	0.781	0.597	0.985	0.703	0.606	0.541	0.887	0.654	0.729	0.597	0.628	0.561	0.887	0.648
	Avg	0.550	0.513	0.669	0.560	0.663	0.540	0.757	0.578	0.726	0.579	0.602	0.530	0.868	0.625	0.576	0.511	0.565	0.513	0.865	0.621
ETTh2 ↓ ETTm1	96	0.204	0.297	0.221	0.303	0.258	0.326	0.253	0.329	0.224	0.306	0.238	0.318	0.244	0.330	0.225	0.310	0.226	0.309	0.248	0.324
	192	0.262	0.332	0.295	0.344	0.303	0.342	0.293	0.346	0.312	0.368	0.293	0.351	0.291	0.356	0.288	0.347	0.289	0.345	0.296	0.352
	336	0.307	0.359	0.340	0.376	0.356	0.383	0.347	0.376	0.351	0.386	0.407	0.422	0.351	0.391	0.350	0.384	0.348	0.379	0.353	0.383
	720	0.394	0.419	0.453	0.428	0.440	0.434	0.446	0.429	0.517	0.490	0.462	0.447	0.452	0.451	0.452	0.441	0.439	0.427	0.471	0.446
	Avg	0.292	0.350	0.327	0.363	0.339	0.371	0.335	0.370	0.351	0.388	0.350	0.385	0.335	0.382	0.329	0.371	0.325	0.365	0.342	0.376
ETTm1 ↓ ETTh2	96	0.327	0.375	0.358	0.382	0.355	0.403	0.353	0.392	0.382	0.406	0.385	0.408	0.371	0.407	0.350	0.383	0.354	0.385	0.377	0.407
	192	0.396	0.414	0.454	0.444	0.449	0.450	0.443	0.444	0.474	0.452	0.499	0.470	0.463	0.458	0.438	0.428	0.447	0.434	0.471	0.453
	336	0.408	0.431	0.488	0.452	0.479	0.467	0.469	0.461	0.585	0.523	0.609	0.529	0.481	0.485	0.463	0.453	0.481	0.463	0.472	0.484
	720	0.423	0.449	0.469	0.478	0.477	0.476	0.466	0.468	0.496	0.482	0.627	0.548	0.503	0.482	0.459	0.459	0.474	0.471	0.495	0.482
	Avg	0.389	0.417	0.442	0.439	0.440	0.449	0.433	0.439	0.484	0.466	0.530	0.489	0.455	0.458	0.428	0.431	0.439	0.438	0.457	0.454
ETTm1 ↓ ETTm2	96	0.177	0.261	0.203	0.299	0.218	0.271	0.217	0.294	0.198	0.275	0.199	0.277	0.219	0.305	0.197	0.269	0.195	0.271	0.222	0.295
	192	0.237	0.303	0.272	0.325	0.288	0.335	0.277	0.327	0.263	0.316	0.269	0.324	0.277	0.347	0.258	0.307	0.258	0.311	0.288	0.337
	336	0.289	0.337	0.303	0.347	0.322	0.355	0.331	0.360	0.328	0.360	0.337	0.366	0.354	0.378	0.317	0.344	0.317	0.348	0.341	0.367
	720	0.368	0.386	0.436	0.418	0.414	0.409	0.429	0.413	0.423	0.409	0.436	0.419	0.426	0.420	0.415	0.399	0.416	0.404	0.436	0.418
	Avg	0.268	0.323	0.304	0.347	0.311	0.343	0.313	0.348	0.303	0.340	0.310	0.347	0.319	0.363	0.297	0.330	0.296	0.334	0.322	0.354
ETTm2 ↓ ETTh2	96	0.298	0.357	0.324	0.383	0.334	0.416	0.360	0.401	0.325	0.370	0.337	0.378	0.347	0.401	0.334	0.376	0.327	0.367	0.360	0.401
	192	0.366	0.399	0.403	0.422	0.439	0.441	0.434	0.437	0.417	0.422	0.414	0.420	0.438	0.444	0.421	0.423	0.411	0.418	0.434	0.437
	336	0.403	0.426	0.434	0.442	0.455	0.457	0.460	0.459	0.437	0.444	0.444	0.448	0.459	0.464	0.459	0.454	0.439	0.447	0.460	0.459
	720	0.419	0.448	0.462	0.467	0.488	0.479	0.485	0.477	0.475	0.479	0.457	0.466	0.485	0.477	0.454	0.460	0.459	0.470	0.485	0.477
	Avg	0.372	0.408	0.406	0.429	0.429	0.448	0.435	0.443	0.414	0.429	0.413	0.428	0.432	0.447	0.417	0.428	0.409	0.425	0.435	0.443
ETTm2 ↓ ETTm1	96	0.448	0.426	0.583	0.524	0.488	0.445	0.747	0.558	0.488	0.444	0.609	0.500	0.619	0.564	0.472	0.447	0.491	0.437	0.747	0.558
	192	0.471	0.446	0.609	0.501	0.555	0.464	0.781	0.560	0.527	0.465	0.677	0.536	0.685	0.565	0.519	0.467	0.530	0.470	0.781	0.560
	336	0.495	0.467	0.585	0.522	0.608	0.538	0.778	0.578	0.572	0.486	0.708	0.558	0.792	0.578	0.531	0.477	0.565	0.497	0.778	0.578
	720	0.568	0.508	0.712	0.579	0.699	0.566	0.769	0.573	0.635	0.528	0.846	0.620	0.727	0.579	0.585	0.506	0.686	0.565	0.769	0.573
	Avg	0.496	0.462	0.622	0.532	0.588	0.503	0.769	0.567	0.556	0.481	0.710	0.554	0.706	0.572	0.527	0.474	0.568	0.492	0.769	0.567
Average		0.375	0.401	0.437	0.431	0.434	0.429	0.472	0.441	0.441	0.430	0.454	0.438	0.492	0.462	0.409	0.413	0.412	0.417	0.492	0.451

Transformer [48], FlowFormer [49]), an MLP-based model (LightTS [52]), and a CNN-based model (TCN [53]). Compared with these baselines across various architectures, our S^2TS-LLM achieves superior performance, demonstrating its strong versatility and representational capacity.

Table 15: Full results for the classification task. '.' indicates the name of *former. A higher value indicates better performance. Red denotes the best performance, while Blue indicates the second-best.

Methods	S²TS-LLM	LLMs			CNNs		MLPs			Transformers							RNNs		Classical Methods	
	(Ours)	S²IP-LLM	Time-LLM	GPT4TS	TimesNet	TCN	TimeMixer	Rlinear	LightTS	TimeXer	iTrans.	PatchTST	Flow.	Non-Station.	In.	Trans.	LSSL	LSTNet	Rocket	XGBoost
EthanolConcentration	44.1	35.3	34.6	34.2	35.7	28.9	25.9	28.5	29.7	28.9	32.3	25.1	33.8	32.7	31.6	32.7	31.1	39.9	45.2	43.7
FaceDetection	69.7	68.5	67.9	69.2	68.6	52.8	67.3	63.4	67.5	69.4	68.5	66.2	67.6	68.0	67.0	67.3	66.7	65.7	64.7	63.3
Handwriting	34.2	33.1	32.0	32.7	32.1	53.3	25.3	22.6	26.1	24.6	31.7	26.8	33.8	31.6	32.8	32.0	24.6	25.8	58.8	15.8
Heartbeat	79.5	77.5	78.0	77.2	78.0	75.6	74.6	64.4	75.1	74.6	75.6	72.2	77.6	73.7	80.5	76.1	72.7	77.1	75.6	73.2
JapaneseVoxels	98.9	98.6	98.1	98.6	98.4	98.9	95.9	96.5	96.2	97.8	98.3	95.7	98.9	99.2	98.9	98.7	98.4	98.1	96.2	86.5
PEMS-SF	90.7	88.4	87.2	87.9	89.6	68.8	87.9	86.1	88.4	79.8	88.4	74.6	83.8	87.3	81.5	82.1	86.1	86.7	75.1	98.3
SelfRegulationSCP1	93.5	91.4	92.8	93.2	91.8	84.6	92.5	86.7	89.8	87.0	90.7	81.9	92.5	89.4	90.1	92.2	90.8	84.0	90.8	84.6
SelfRegulationSCP2	62.2	58.3	57.2	59.4	57.2	55.6	56.7	52.8	51.1	53.3	56.6	53.3	56.1	57.2	53.3	53.9	52.2	52.8	53.3	48.9
SpokenArabicDigits	99.8	99.9	99.5	99.2	99.2	95.6	99.1	95.9	100.0	98.5	100.0	97	98.8	100.0	100.0	98.4	100.0	100.0	71.2	69.6
UWaveGestureLibrary	91.9	88.7	89.3	88.1	85.3	88.4	83.4	75.6	80.3	84.1	82.5	81.6	86.6	87.5	85.6	85.6	85.9	87.8	94.4	75.9
Average	76.4	73.9	73.7	74.0	73.6	70.3	70.9	67.2	70.4	69.8	72.5	67.4	73.0	72.7	72.1	71.9	70.9	71.8	72.5	66.0

Table 16: Full MSE results of ablation Study on the ETTh1 and ETTh2 datasets. A lower value indicates better performance. Red denotes the best performance, while Blue indicates the second-best.

Dataset		**S²TS-LLM**	(Q1) Component Contribution			(Q2) Scalability		(Q3) LLM Effectiveness		
		(Ours)	**w/o Symbol**	**w/o Segment**	**w/o Fusion**	**w Vocab**	**w BERT**	**w/o Pretrain**	**w Att**	**w Trans**
ETTh1	96	0.355±0.009	0.361±0.001	0.361±0.001	0.356±0.003	0.351±0.003	0.360±0.001	0.368±0.002	0.388±0.004	0.384±0.003
	192	0.399±0.001	0.403±0.001	0.403±0.001	0.401±0.005	0.398±0.003	0.398±0.003	0.429±0.001	0.420±0.007	0.411±0.006
	336	0.402±0.004	0.432±0.015	0.431±0.005	0.415±0.003	0.401±0.005	0.404±0.002	0.452±0.005	0.437±0.012	0.433±0.004
	720	0.463±0.001	0.477±0.026	0.468±0.003	0.479±0.015	0.464±0.001	0.467±0.006	0.488±0.007	0.489±0.030	0.467±0.020
	Avg	0.404±0.003	0.418±0.010	0.416±0.002	0.413±0.002	0.403±0.002	0.407±0.002	0.434±0.002	0.432±0.009	0.424±0.005
ETTh2	96	0.260±0.003	0.274±0.004	0.275±0.003	0.269±0.005	0.261±0.002	0.257±0.001	0.275±0.002	0.298±0.002	0.291±0.003
	192	0.312±0.004	0.335±0.005	0.338±0.004	0.319±0.004	0.311±0.002	0.313±0.001	0.347±0.004	0.362±0.006	0.364±0.001
	336	0.322±0.001	0.336±0.001	0.339±0.001	0.321±0.003	0.321±0.004	0.319±0.001	0.360±0.001	0.366±0.004	0.359±0.003
	720	0.392±0.002	0.406±0.005	0.408±0.006	0.408±0.005	0.394±0.004	0.394±0.004	0.403±0.004	0.426±0.016	0.419±0.008
	Avg	0.321±0.002	0.345±0.003	0.347±0.003	0.329±0.003	0.321±0.003	0.321±0.001	0.346±0.003	0.362±0.005	0.356±0.001

E.6 Ablation Study

We conduct an ablation study with eight model variants on the ETTh1 and ETTh2 datasets to address the following questions: **(Q1)** *Do individual components contribute meaningfully to the framework?* **(Q2)** *How scalable is the framework?* and **(Q3)** *Are LLMs effective for time series tasks?* Table 16 reports the detailed ablation results using the MSE metric, averaged over three runs.

To answer Q1, we design the following three variants of S^{2}TS-LLM, including "w/o Symbol", "w/o Segment", and "w/o Fusion":

- **"w/o Symbol":** Removes the spectral symbolization component (Section 3.2), meaning the model does not learn textual abstractions to align time series with natural language in the representation space.
- **"w/o Segment":** Removes the contextual segmentation component (Section 3.3), meaning the model does not learn segment-level positions for aligning temporal structures with natural language contexts.
- **"w/o Fusion":** Replaces our time-linguistic fusion strategy (Section 3.4) with a simple summation of the temporal and textual LLM outputs.

As shown in Table 16, removing either the spectral symbolization or contextual segmentation leads to performance drops, as they disrupt the knowledge transferring from natural language to time series. This highlights the necessity of both components in enabling LLMs to comprehend temporal semantics and structural relationships. Additionally, the inferior performance of "w/o Fusion" variant indicates the effectiveness of our fusion strategy in bridging the representational gap between time series and natural language.

Regarding Q2, we design two variants of S^{2}TS-LLM, including "w Vocab" and "w BERT", to evaluate the scalability of the symbolic representation and the adaptability of different LLM architectures:

- **"w Vocab":** Replaces ASCII symbols with vocabulary for textual abstracting. Specifically, we query LLMs to select 24 vocabulary terms that are well-suited for describing frequency characteristics, including trend, daily, harmonic, peak, rhythm, cycle, noise, disturbance, pattern, pulse, beat, fluctuation, seasonality, vibration, waveform, instability, perturbation, anomaly, impulse, oscillation, turbulence, interference, variation, and echo.

- **“w BERT”:** Substitutes GPT-2 with BERT [47] as the backbone LLM. Both GPT-2 and BERT have comparable sizes (12 Transformer layers, 124M vs. 110M parameters). Following our GPT-2 setup, we utilize the first 4 layers of BERT for time series analysis.

As shown in Table 16, the **“w Vocab”** setting can yield accurate and stable predictions, because vocabulary-based representations describe frequency patterns more precisely than ASCII symbols. While the “w Vocab” variant uses general vocabulary terms for frequency descriptions, we believe that customizing the word set for specific datasets could further enhance performance. However, this approach requires prior knowledge and could introduce substantial preprocessing overhead as the vocabulary size grows. Additionally, the **“w BERT”** variant achieves competitive results relative to the default GPT-2 used in S^{2}TS-LLM, demonstrating the scalability and flexibility of our framework.

Finally, to address Q3, we design three variants by removing the LLM from our framework:

- **“w/o Pretrain”:** Initializes the LLM parameters randomly, without any pre-training.
- **“w Att”:** Replaces the GPT-2 backbone with a single Attention layer.
- **“w Trans”:** Substitutes the GPT-2 backbone with a single Transformer layer.

All three variants discard the prior knowledge of pre-trained LLMs, resulting in the poorest performance among all settings. These results highlight the importance of leveraging LLMs for time series analysis, as their ability to model long-range dependencies and their rich internal knowledge facilitate the effective extraction of periodic patterns and comprehension of multimodal data [20].